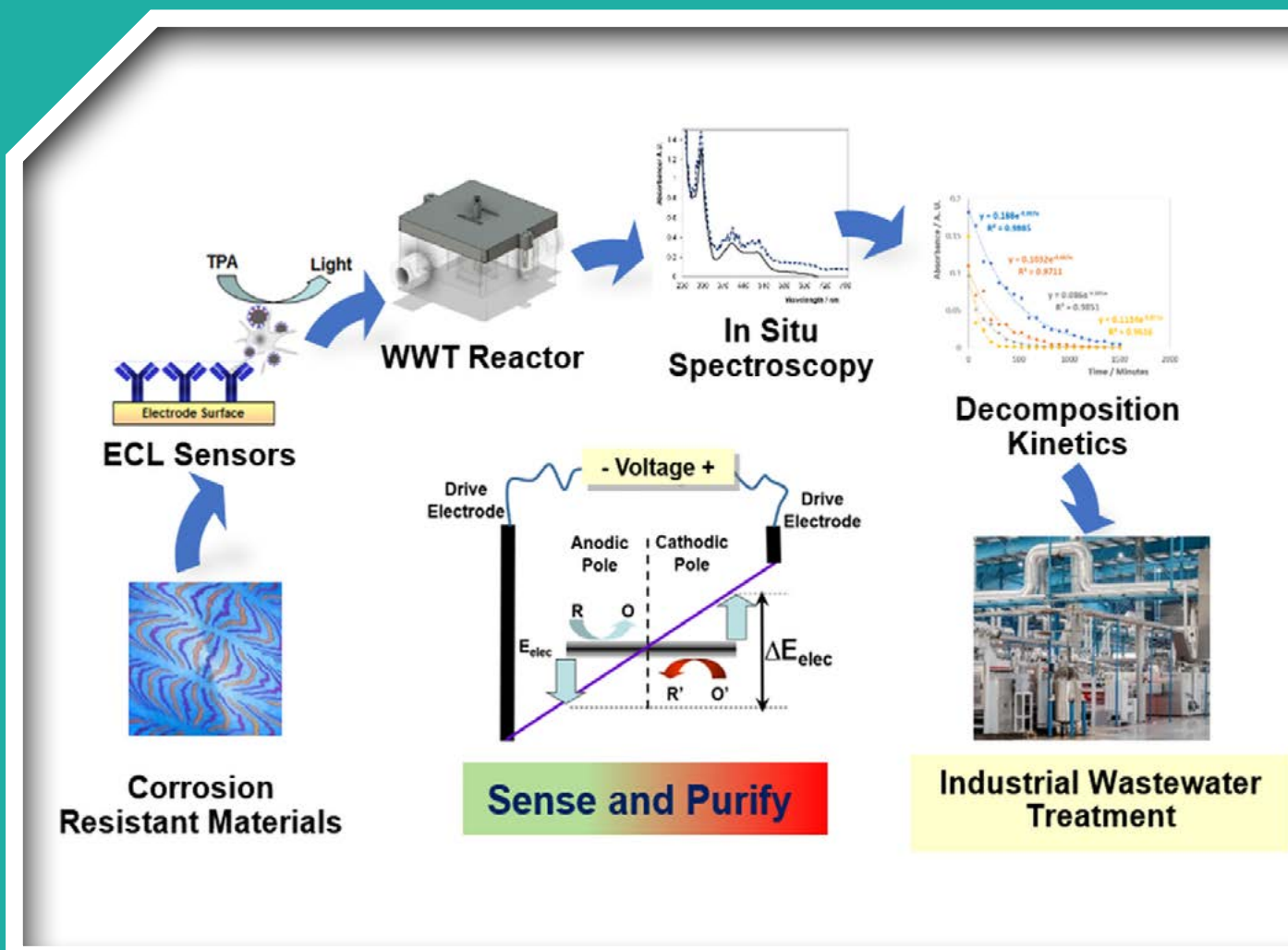


# Sense and Purify (SPy): Detect, Destroy and Remove Water Contaminants

Authors: Robert J. Forster



# Environmental Protection Agency

The EPA is responsible for protecting and improving the environment as a valuable asset for the people of Ireland. We are committed to protecting people and the environment from the harmful effects of radiation and pollution.

## The work of the EPA can be divided into three main areas:

**Regulation:** Implementing regulation and environmental compliance systems to deliver good environmental outcomes and target those who don't comply.

**Knowledge:** Providing high quality, targeted and timely environmental data, information and assessment to inform decision making.

**Advocacy:** Working with others to advocate for a clean, productive and well protected environment and for sustainable environmental practices.

## Our Responsibilities Include:

### Licensing

- > Large-scale industrial, waste and petrol storage activities;
- > Urban waste water discharges;
- > The contained use and controlled release of Genetically Modified Organisms;
- > Sources of ionising radiation;
- > Greenhouse gas emissions from industry and aviation through the EU Emissions Trading Scheme.

### National Environmental Enforcement

- > Audit and inspection of EPA licensed facilities;
- > Drive the implementation of best practice in regulated activities and facilities;
- > Oversee local authority responsibilities for environmental protection;
- > Regulate the quality of public drinking water and enforce urban waste water discharge authorisations;
- > Assess and report on public and private drinking water quality;
- > Coordinate a network of public service organisations to support action against environmental crime;
- > Prosecute those who flout environmental law and damage the environment.

### Waste Management and Chemicals in the Environment

- > Implement and enforce waste regulations including national enforcement issues;
- > Prepare and publish national waste statistics and the National Hazardous Waste Management Plan;
- > Develop and implement the National Waste Prevention Programme;
- > Implement and report on legislation on the control of chemicals in the environment.

### Water Management

- > Engage with national and regional governance and operational structures to implement the Water Framework Directive;
- > Monitor, assess and report on the quality of rivers, lakes, transitional and coastal waters, bathing waters and groundwaters, and measurement of water levels and river flows.

### Climate Science & Climate Change

- > Publish Ireland's greenhouse gas emission inventories and projections;

- > Provide the Secretariat to the Climate Change Advisory Council and support to the National Dialogue on Climate Action;
- > Support National, EU and UN Climate Science and Policy development activities.

### Environmental Monitoring & Assessment

- > Design and implement national environmental monitoring systems: technology, data management, analysis and forecasting;
- > Produce the State of Ireland's Environment and Indicator Reports;
- > Monitor air quality and implement the EU Clean Air for Europe Directive, the Convention on Long Range Transboundary Air Pollution, and the National Emissions Ceiling Directive;
- > Oversee the implementation of the Environmental Noise Directive;
- > Assess the impact of proposed plans and programmes on the Irish environment.

### Environmental Research and Development

- > Coordinate and fund national environmental research activity to identify pressures, inform policy and provide solutions;
- > Collaborate with national and EU environmental research activity.

### Radiological Protection

- > Monitoring radiation levels and assess public exposure to ionising radiation and electromagnetic fields;
- > Assist in developing national plans for emergencies arising from nuclear accidents;
- > Monitor developments abroad relating to nuclear installations and radiological safety;
- > Provide, or oversee the provision of, specialist radiation protection services.

### Guidance, Awareness Raising, and Accessible Information

- > Provide independent evidence-based reporting, advice and guidance to Government, industry and the public on environmental and radiological protection topics;
- > Promote the link between health and wellbeing, the economy and a clean environment;
- > Promote environmental awareness including supporting behaviours for resource efficiency and climate transition;
- > Promote radon testing in homes and workplaces and encourage remediation where necessary.

### Partnership and Networking

- > Work with international and national agencies, regional and local authorities, non-governmental organisations, representative bodies and government departments to deliver environmental and radiological protection, research coordination and science-based decision making.

## Management and Structure of the EPA

The EPA is managed by a full time Board, consisting of a Director General and five Directors. The work is carried out across five Offices:

1. Office of Environmental Sustainability
2. Office of Environmental Enforcement
3. Office of Evidence and Assessment
4. Office of Radiation Protection and Environmental Monitoring
5. Office of Communications and Corporate Services

The EPA is assisted by advisory committees who meet regularly to discuss issues of concern and provide advice to the Board.

# Sense and Purify (SPy): Detect, Destroy and Remove Water Contaminants

Authors: Robert J. Forster

## Identifying pressures

Many wastewater streams, for example from the pharmaceutical and food industries or from municipal wastewater, contain pollutants. These include active pharmaceutical ingredients, herbicides, pesticides and, increasingly, personal care products, which cannot be efficiently removed or broken down with conventional primary, secondary (biological) and tertiary treatments. Moreover, the current practice of “pooling” wastewater from many different sources and treating centrally is not ideal, since the treatment method cannot easily be optimised to address the different pollutants present. There is growing recognition that powerful treatments are needed that can process diverse biological and synthetic organic compounds, and can be implemented at the point of production. Our work focused on advanced oxidation processes (AOPs) that can degrade and even mineralise recalcitrant organic matter from wastewater through reaction with hydroxyl radicals using sustainably generated electricity.

## Informing policy

The eco-innovative ‘Sense and Purify’ (SPy) technology, developed by the project, has significant advantages over traditional treatment processes, including low operations costs, significantly lower energy consumption, higher conversion efficiency, better effluent water quality and lower waste production.

From a policy perspective, SPy technology could make it easier to comply with environmental regulations and standards for wastewater treatment. It has proven effective at removing persistent pollutants, such as pharmaceuticals, personal care products and endocrine-disrupting compounds, which can be difficult to remove using conventional wastewater treatment processes. The use of AOPs can help wastewater treatment plants to comply with regulations and standards for discharge of treated wastewater into surface waters.

From a societal perspective, SPy’s findings can help to protect public health and the environment by removing contaminants from wastewater that could potentially harm human health or aquatic life. This can help to ensure that treated wastewater is safe for discharge into surface waters or for reuse in non-potable applications.

From a commercial perspective, the demand for wastewater treatment services is increasing significantly and the market for AOPs and other advanced treatment technologies is growing.

## Developing solutions

SPy technology allows organic molecules and pathogens to be decomposed and mineralised to carbon dioxide, ammonia and water, by generating a high concentration of a powerful oxidising agent, hydroxyl radicals, throughout a water sample with high electrical efficiency. The active agent has no persistent toxicity and can be implemented at source. It is also highly mobile/portable, low cost, compatible with flow-through reactor design, energy efficient and environmentally friendly. A laboratory-scale prototype reactor was developed that uses titanium feeder electrodes to generate an electric field that allows the voltage of boron-doped diamond (BDD) particles in suspension to be controlled. By controlling electrode separation, the voltage applied to the feeder electrodes and BDD particle size, the BDD particles suspended in the wastewater produce hydroxyl radicals that then decompose the organic pollutants. To monitor the decomposition of organics, UV-Vis spectroscopy was used. The absorbance correlates well with total organic carbon content. The system was tested for the treatment of pharmaceutical wastewater and is capable of mineralising non-steroidal anti-inflammatory and anti-cancer drugs within 1–5 hours.

**EPA RESEARCH PROGRAMME 2021–2030**

# **Sense and Purify (SPy): Detect, Destroy and Remove Water Contaminants**

**(2019-W-MS-41)**

## **EPA Research Report**

Prepared for the Environmental Protection Agency

by

Dublin City University

**Author:**

**Robert J. Forster**

**ENVIRONMENTAL PROTECTION AGENCY**  
An Ghníomhaireacht um Chaomhnú Comhshaoil  
PO Box 3000, Johnstown Castle, Co. Wexford, Ireland

Telephone: +353 53 916 0600 Fax: +353 53 916 0699  
Email: [info@epa.ie](mailto:info@epa.ie) Website: [www.epa.ie](http://www.epa.ie)

## **ACKNOWLEDGEMENTS**

This report is published as part of the EPA Research Programme 2021–2030. The EPA Research Programme is a Government of Ireland initiative funded by the Department of the Environment, Climate and Communications. It is administered by the Environmental Protection Agency, which has the statutory function of co-ordinating and promoting environmental research. The programme was jointly funded under the Water JPI 2018 Joint Call (WaterWorks2017).

The authors would like to acknowledge the members of the project steering committee, namely Paul Butler, Enterprise Ireland; Greg Beechinor, EPA; and Edmond O’Reilly, Irish Water. The outstanding programme management expertise and inspirational support of Oonagh Monahan (Research Project Manager on behalf of the EPA) and Lisa Shiels (EPA) played a central role in progressing this project and are sincerely appreciated.

## **DISCLAIMER**

Although every effort has been made to ensure the accuracy of the material contained in this publication, complete accuracy cannot be guaranteed. The Environmental Protection Agency, the author and the steering committee members do not accept any responsibility whatsoever for loss or damage occasioned, or claimed to have been occasioned, in part or in full, as a consequence of any person acting, or refraining from acting, as a result of a matter contained in this publication. All or part of this publication may be reproduced without further permission, provided the source is acknowledged.

This report is based on research carried out/data from 1 April 2019 to 31 October 2022. More recent data may have become available since the research was completed.

The EPA Research Programme addresses the need for research in Ireland to inform policymakers and other stakeholders on a range of questions in relation to environmental protection. These reports are intended as contributions to the necessary debate on the protection of the environment.

**EPA RESEARCH PROGRAMME 2021–2030**  
Published by the Environmental Protection Agency, Ireland

ISBN: 978-1-80009-103-0

June 2023

Price: Free

Online version

## Project Partners

**Professor Yann Pellegrin**

Nantes University

Nantes

France

Tel.: +33 276 645 174

Email: Yann.Pellegrin@univ-nantes.fr

**Professor Ciara O’Sullivan**

Universitat Rovira i Virgili

Tarragona

Spain

Tel.: +34 977 559 651

Email: ciara.osullivan@urv.cat

**Professor Emmanuel Iwuoha**

University of the Western Cape

Cape Town

South Africa

Tel.: +27 21 959 3060

Email: eiwuoha@uwc.ac.za



# Contents

<b>Acknowledgements</b>	<b>ii</b>
<b>Disclaimer</b>	<b>ii</b>
<b>Project Partners</b>	<b>iii</b>
<b>List of Figures</b>	<b>vi</b>
<b>List of Tables</b>	<b>ix</b>
<b>Executive Summary</b>	<b>xi</b>
<b>1 Introduction</b>	<b>1</b>
1.1 Challenge	1
1.2 Overview	1
1.3 Objectives	2
<b>2 Overview of the Research</b>	<b>3</b>
<b>3 Examination of the Findings</b>	<b>4</b>
3.1 Work Package 1: Sensors for Wastewater	4
3.2 Work Package 2: Optimised Particles for Wastewater Treatment	11
3.3 Work Package 3: Integrated Reactor	14
3.4 Work Package 4: Real-world Wastewater Testing	18
<b>4 Conclusions and Policy Recommendations</b>	<b>26</b>
4.1 Target Markets Identified	26
<b>References</b>	<b>28</b>
<b>Abbreviations</b>	<b>29</b>



## List of Figures

Figure 1.1.	Electro-Fenton system for the degradation of organic pollutants in water	1
Figure 2.1.	Wireless electrochemical cell showing linear voltage drop generated by two external, electrically isolated, drive electrodes	3
Figure 3.1.	Schematic of the immunosensors developed	4
Figure 3.2.	Screen-printed electrodes (22 individual sensor platforms are shown)	4
Figure 3.3.	Cyclic voltammograms of a 5 mM solution of ferrocene methanol at an SPy screen-printed electrode	5
Figure 3.4.	Poly(NIPAM) polymer used for covalent attachment of pathogen antibodies in a 3D layer on electrodes	5
Figure 3.5.	Confocal fluorescence microscopy image of NIPAM polymer film deposited on an electrode following conjugation of FITC-labelled Gram-negative antibodies	6
Figure 3.6.	Z-stack confocal fluorescence microscopy image of NIPAM polymer film deposited on an electrode following conjugation of FITC-labelled Gram-negative antibodies	6
Figure 3.7.	(A) <i>E. coli</i> captured on a glassy carbon electrode functionalised with a 550 nm thick polypyrrole film containing capture antibodies for <i>E. coli</i> . (B) Captured <i>E. coli</i> when a voltage of 0.5 V is applied. (C) Removal of captured <i>E. coli</i> when a voltage of +1.0 V is applied so as to oxidise the polypyrrole film. (D) Rebinding of <i>E. coli</i> when the electrode is returned to open circuit	6
Figure 3.8.	Highly sensitive sensor for the detection and quantification of <i>E. coli</i> in water based on the generation of ECL when a voltage is applied	7
Figure 3.9.	Integrated sensor platform that incorporates an Ag/AgCl reference electrode as well as carbon counter and working electrodes	7
Figure 3.10.	Dependence of the ECL intensity on the concentration of <i>E. coli</i> in a water sample	7
Figure 3.11.	High-brightness silicate nanoparticles loaded with ruthenium complexes	8
Figure 3.12.	ECL from a 1 $\mu$ M suspension of silicate nanoparticles loaded with a ruthenium poly-pyridyl complex	8
Figure 3.13.	Dependence of the ECL intensity on the concentration of <i>E. coli</i> in a water sample	8
Figure 3.14.	Dependence of the ECL light intensity on the concentration of atrazine in an antibody sandwich assay	9

Figure 3.15.	Relationship between the pathogen concentration measured using sampling and <i>ex situ</i> analysis ( <i>y</i> -axis) and that determined when the sensor is placed inside the reactor	9
Figure 3.16.	UV-Vis spectra of the blank electrolyte solution (Blanc_Na <sub>2</sub> SO <sub>4</sub> ) and the parent drug doxorubicin (DOX), and after degradation using electrogenerated hydroxyl radicals for 30, 60, 90 and 120 minutes	10
Figure 3.17.	UV-Vis spectra of a pharma wastewater stream in the SPy reactor	10
Figure 3.18.	Correlation of gemcitabine concentration as determined using UV-Vis spectroscopy with traditional TOC measurement	10
Figure 3.19.	Calculated concentration–distance profiles of hydroxyl radicals during oxidation of (1) 1.0 M, (2) 0.75 M, (3) 0.5 M and (4) 0.25 M gemcitabine	11
Figure 3.20.	Prediction of the electric field distribution through solution using COMSOL Multiphysics software	12
Figure 3.21.	Formation of fluorescent 7OHC from coumarin using electrogenerated hydroxyl radicals	12
Figure 3.22.	Cyclic voltammograms of BDD materials with boron concentrations of (A) $2 \times 10^{21}$ atoms cm <sup>-3</sup> and (B) $5 \times 10^{20}$ atoms cm <sup>-3</sup>	13
Figure 3.23.	Cyclic voltammograms of BDD electrodes with a boron concentration of $5 \times 10^{20}$ atoms cm <sup>-3</sup>	13
Figure 3.24.	Ratio of the concentrations of adriamycin decomposed to the radical produced as a function of the voltage	13
Figure 3.25.	Flow of wastewater stream through the SPy reactor	14
Figure 3.26.	(A) SPy reactor featuring a pair of feeder electrodes. (B) Photograph of reactor that was 3D printed using PETG	15
Figure 3.27.	Schematic of flow-through reactor for wireless treatment of wastewater	15
Figure 3.28.	Upper electrode is a pristine titanium electrode and the lower electrode is a titanium electrode following oxidation at +1.8 V for 300 s	17
Figure 3.29.	Photograph of the screen-printed carbon-based electrode tested as a feeder electrode in the SPy reactor	17
Figure 3.30.	Structure of the anti-neoplastic drug doxorubicin	18
Figure 3.31.	UV-Vis spectra of the blank electrolyte solution, the parent drug doxorubicin and during degradation using electrogenerated hydroxyl radicals	19
Figure 3.32.	Structure of the anti-cancer drug gemcitabine	19
Figure 3.33.	Changes in (A) UV-Vis spectra and (B) HPLC traces of a 1 mM solution of gemcitabine following electrolysis in the SPy reactor using BDD particles to wirelessly generate hydroxyl radicals for periods of 0, 1, 2, 3, 4 and 5 hours (top to bottom at 270 nm)	20
Figure 3.34.	Structure of fluorinated gemcitabine	20

Figure 3.35.	Changes in the UV-Vis spectra of a 1 mM solution of fluorinated gemcitabine following electrolysis in the SPy reactor using BDD particles to wirelessly generate hydroxyl radicals for periods of 0, 1, 2, 3, 4 and 5 hours (top to bottom at 270 nm)	20
Figure 3.36.	Structure of the blood thinner warfarin	20
Figure 3.37.	Electrolysis of coumadin (10 mM warfarin) dissolved in Milli-Q water for (A) 45 minutes, (B) 90 minutes and (C) 270 minutes	21
Figure 3.38.	Decrease in absorbance at 270 nm of a 0.9 mM solution of fluorinated gemcitabine (blue), doxorubicin (orange) and cabometyx (grey) in Milli-Q water over time during wireless electrochemical incineration	21
Figure 3.39.	Changes in the UV-Vis of a first-wash sample following treatment in the SPy reactor for periods of 0, 1, 2 and 3 hours (top to bottom at 500 nm)	21
Figure 3.40.	Changes in absorbance at 550 nm over time during the treatment of a first-wash sample	22
Figure 3.41.	Structure of pectin, a significant component of wastewater associated with fruit processing	22
Figure 3.42.	Decrease in absorbance at 280 nm of a 10 mM solution of pectin in Milli-Q water over time during wireless electrochemical incineration	23
Figure 3.43.	(A) Differential pulse voltammograms of 5 $\mu\text{g ml}^{-1}$ NVP at different pH values (7–12) recorded in a BDD reactor. (B) Dependence of the peak potential, $E_p$ , on the solution pH from pH 7 to pH 10 (main) and from pH 10 to pH 12 (inset)	25
Figure 3.44.	Proposed mechanism for electrooxidation of NVP in alkaline media in a BDD reactor	25

## List of Tables

Table 3.1.	Composition of the ink used to screen-print electrodes to act as feeder electrodes in the SPy prototype reactor	17
------------	-----------------------------------------------------------------------------------------------------------------	----



# Executive Summary

“Sense and Purify” technology allows organic molecules and pathogens, which are difficult to remove or decompose using conventional wastewater treatments, to be decomposed and ultimately mineralised to carbon dioxide, ammonia and water. It does this by generating a high concentration of a powerful oxidising agent, hydroxyl radicals, throughout a water sample with very high electrical efficiency. The oxidising agent has no persistent toxicity (radical lifetime is  $\approx 5 \mu\text{s}$ ), can be implemented at source, and is highly mobile/portable, low cost, compatible with flow-through reactor design, energy efficient and environmentally friendly.

A laboratory-scale prototype reactor ( $100 \text{ cm}^3$ ) has been developed that uses titanium feeder electrodes to generate an electric field that allows the voltage of a suspension of boron-doped diamond (BDD) particles in suspension to be controlled. With the optimum electrode separation, voltage applied to the feeder electrodes and BDD particle size, the BDD particles suspended in the wastewater become polarised to 1.5 V and hydroxyl radicals are produced that then decompose the organic pollutants. The optimum BDD particle size is 1–3 mm with a boron doping level of  $5 \times 10^{20} \text{ atoms cm}^{-3}$ .

Antibody sensors for *Escherichia coli* bacteria have been developed based on electrochemiluminescence detection and are capable of detecting bacteria at  $> 100 \text{ colony-forming units cm}^{-3}$ . However, the materials within these sensors, especially the antibodies, decompose rapidly when placed inside the reactor

because of the hydroxyl radicals present. Therefore, to monitor the decomposition of the organic materials present, UV-Vis spectroscopy was used and the absorbance correlates well with the total organic carbon. The system has been tested for the treatment of pharmaceutical wastewater and is capable of mineralising non-steroidal anti-inflammatory drugs and anti-cancer drugs within 1–5 hours. In samples of this type, which contain a limited number of well-defined organic materials with a low overall level of total organic carbon, anodised titanium feeder electrodes are stable for operating periods of several tens of hours without functional loss. However, in samples that have a high organic carbon content and a diverse range of contaminants, e.g. wastewater from food processing, the titanium feeder electrodes corrode over a period of 1–5 hours, even after protection with an oxide coating. This behaviour is strongly related to the presence of metal ion chelators, e.g. polyphenols and pectin, in these samples.

Although identifying the optimum sector for the application of this technology requires additional research, we have produced two reports, the first addressing the issues involved in the practical deployment of the technology and a second looking at the potential route to commercialisation. In conclusion, the technical objectives of the programme have been reached and a prototype reactor has been developed that is capable of decomposing recalcitrant organic materials, notably active pharmaceutical ingredients, within a relatively short period of time.



# 1 Introduction

## 1.1 Challenge

The outlook for water is sobering. The ever-expanding demand for water by the world's growing population and economy, combined with the impacts of climate change, is already causing shortages, damaging livelihoods, and compromising the health of people and ecosystems. By 2035, demand for water will be 40% higher than it is today. Treating and recycling wastewater, especially industrial wastewater, needs to be a key aspect of closing the water gap. However, many wastewater streams, e.g. from the pharmaceutical and food industries as well as municipal wastewater, contain pollutants, e.g. active pharmaceutical ingredients (APIs) and precursors, herbicides, pesticides and, increasingly, personal care products, that cannot be efficiently removed or broken down with conventional primary, secondary (biological) and tertiary treatments. Moreover, the current practice of "pooling" wastewater from many different municipal and industrial sources and treating centrally is not optimum, since the treatment method cannot be easily optimised to address the different pollutants present. There is growing recognition that what is needed are powerful treatment methods that can process diverse biological and synthetic organic compounds and be implemented at the point of production. For example, pharmaceuticals, including antibiotics (e.g. ciprofloxacin amoxicillin, sulfamethoxazole, tetracycline and erythromycin), non-steroidal anti-inflammatory drugs (NSAIDs) (e.g. ibuprofen, naproxen and aspirin), neuroleptics (e.g. fluphenazine, clozapine and chlorpromazine), oestrogens (e.g. progynova and diethylstilbestrol) and cholesterol-modifying drugs (e.g. atorvastatin and lovastatin), are an increasing issue in various water samples, with concentrations ranging from several nanograms to several micrograms per litre (Vlyssides *et al.*, 2000). Advanced oxidation processes (AOPs) are considered an excellent approach to addressing this issue, either on their own or as part of a wastewater treatment strategy that includes more conventional technologies (Zhang *et al.*, 2021). For example, electrochemical anodic oxidation of ibuprofen containing solutions using Ti/Pt/PbO<sub>2</sub> or boron-doped diamond (BDD) anodes in a conventional electrochemical cell resulted

in decreases in the chemical oxygen demand and total organic carbon (TOC) values of 60%–95% and 48%–92%, respectively, within 6 hours, with higher values being obtained with the BDD electrode (Cirifaco *et al.*, 2009).

## 1.2 Overview

AOPs use electrochemically generated radicals, such as hydroxyl radicals (OH<sup>•</sup>), to oxidise and chemically decompose organic pollutants. The technology is broadly applicable to diverse sectors, including the industrial, pharmaceutical, food and municipal waste sectors. While the objective is to "mineralise" or "electrochemically incinerate" the pollutants within the water, AOPs at a minimum seek to facilitate (post-) treatment processes by creating decomposition products that are more susceptible to bioremediation, are less toxic and have a lower pollutant load. Traditional electrochemical AOP systems, such as that illustrated in Figure 1.1, are environmentally friendly, since green electricity can be used rather than industrial chemicals (Miklos *et al.*, 2018; Sillanpää *et al.*, 2018). The environmental positives are further amplified by high reaction rates and efficiencies, as well as the lack of highly toxic by-products (Katheresan *et al.*, 2018). Hydroxyl radicals are capable of degrading and mineralising highly toxic and complex pollutants because of their high oxidising power (second only to fluorine) and fast oxidation kinetics for mineralisation to CO<sub>2</sub> or to other harmless or beneficial

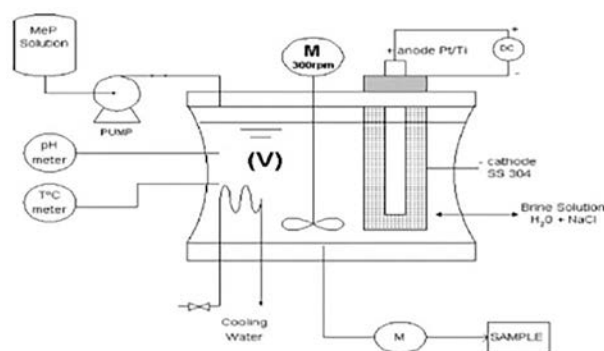


**Figure 1.1. Electro-Fenton system for the degradation of organic pollutants in water.**



by-products, e.g. low-molecular-weight acids that can be used as feedstock for other processes (Prousek, 1996). This area has been the subject of some high-quality reviews (see, for example, Garcia-Costa *et al.*, 2021; Pavlos *et al.*, 2022).

### 1.3 Objectives

The Sense and Purify (SPy) programme set out the following four objectives:

1. **Sensors for wastewater** (Work Package 1). The first objective was to develop rapidly responding, low-cost, highly sensitive detection methods/sensors for pathogens and recalcitrant organic materials, such as pharmaceuticals.
2. **Optimised particles for wastewater treatment** (Work Package 2). The second objective was to optimise the performance of BDD particles to enable a wide range of cellular and organic pollutants to be decomposed and ideally converted to CO<sub>2</sub>, NH<sub>3</sub> and H<sub>2</sub>O.
3. **Integrated reactor** (Work Package 3). The third objective was to use rapid prototyping techniques, including 3D printing/additive manufacturing, to create a reactor capable of testing and treating wastewater. Its performance, based on, for example, water quality at outlet, sample throughput, energy costs and capital costs, was optimised using samples whose composition reflect significant EU and global water challenges and commercial opportunities.
4. **Real-world wastewater testing** (Work Package 4). Finally, the fourth objective was to work closely with industry beneficiaries and test the performance of the reactor using water samples from the Irish pharmaceutical industry.

## 2 Overview of the Research

Electrochemical generation represents a powerful way forward in wastewater treatment and also opens up the possibility of using sustainable energy produced locally from wind or solar. However, pollutants are decomposed only on the electrode surface and therefore must be transported, e.g. using the stirred reactor shown in Figure 1.1, to the electrode surface. This means that high-throughput processing is hard to achieve, especially at scale. Most importantly, in traditional approaches, each electrode is physically wired to a power supply, adding complexity when trying to multiplex electrodes to efficiently treat a large volume of water per unit of time.

To achieve high-throughput processing, the SPy programme has developed a “wireless” electrochemical approach for the mineralisation of recalcitrant organic materials in industrial wastewater. Unlike existing approaches, its key innovation is to use a large number of BDD particles dispersed in the wastewater so that electrochemical oxidation occurs throughout the entire volume of the wastewater sample. Significantly, as shown in Figure 2.1, when an appropriate electric field is applied, each BDD particle acts as a separate electrochemical cell, with hydroxyl radicals being produced on one side and oxygen or water being reduced on the other. Thus, oxidation and reduction are intrinsically linked, and the quantity of electricity consumed during the degradation of the organic pollutants is minimised. The eco-innovative SPy technology has significant advantages over traditional treatment processes, including lower capital, operation and maintenance costs, lower energy

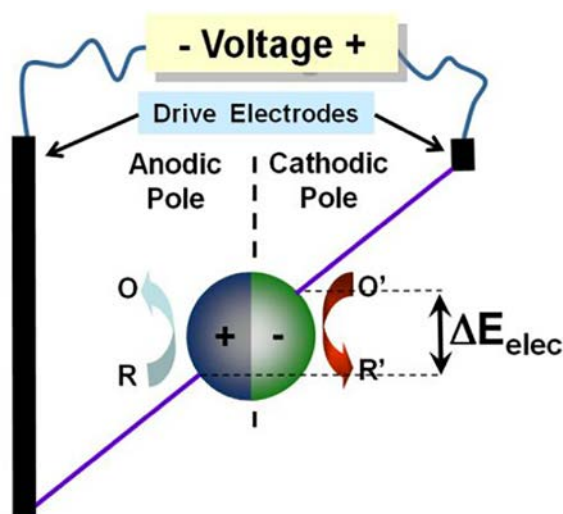


**Figure 2.1. Wireless electrochemical cell showing linear voltage drop generated by two external, electrically isolated, drive electrodes. Either side of the conducting particle assumes a positive or negative potential. Hydroxyl radicals are created from the oxidation of water and these then destroy organic contaminants.**

consumption, higher conversion efficiency, easier operation, better effluent water quality and less waste production. To accelerate and enhance its industrial relevance, the performance of this technology in treating wastewater samples from the pharmaceutical and food industries, as well as municipal waste, has been tested. These experiments have been very insightful regarding deployment and operational issues surrounding the prototype reactor.

### 3 Examination of the Findings

#### 3.1 Work Package 1: Sensors for Wastewater

##### 3.1.1 Task 1.1: in-reactor pathogen sensing – developing sensitive sensors for pathogens in wastewater

The objective of Task 1.1 was to develop a highly sensitive sample-to-answer microfluidic device capable of detecting <100 pathogens per ml within 10 minutes.

As illustrated in Figure 3.1, our approach to detecting pathogens and specific pollutants of interest, e.g. pesticides, involves an electrode platform on which a capture antibody is immobilised and to which, following capture of the target analyte, a detection antibody, with either an electrochemical or electrochemiluminescent label, binds. The intensity of the current or light produced depends on the concentration of the target. First, the fabrication and characterisation of the electrode platforms are described. Second, the selection of the antibodies and their immobilisation are discussed. Third, the performance of the assays for pathogens and a

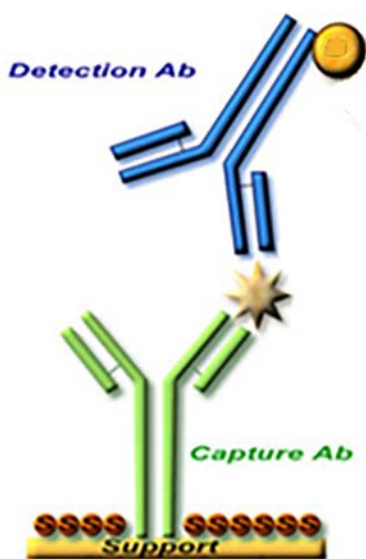


Figure 3.1. Schematic of the immunosensors developed. The detection antibody (Ab) is functionalised with an electrochemical or electrochemiluminescent label.

representative pesticide, atrazine (with a World Health Organization (WHO) guideline value of 100 µg/litre and a WHO acceptable daily intake value of 0–0.02 mg/kg), is presented.

##### *Fabrication and characterisation of screen-printed electrodes*

Low-cost, highly sensitive screen-printed electrodes were produced and used to act as platforms for sensors to detect pathogens in wastewater before treatment and to confirm successful destruction of pathogens after treatment. Specifically, carbon-based inks were formulated and, as shown in Figure 3.2, used to create screen-printed electrodes. The performance of these electrodes was tested using cyclic voltammetry. Figure 3.3 shows voltammetry of ferrocene methanol in an aqueous electrolyte as an electroactive probe. Well-defined peaks associated with the oxidation and reduction of the ferrocene centres can be clearly seen. The theoretical fits of these data (open triangles and open circles) closely match the experimental results observed, indicating that the performance of these screen-printed electrodes is very close to ideal, i.e. the peak-to-peak

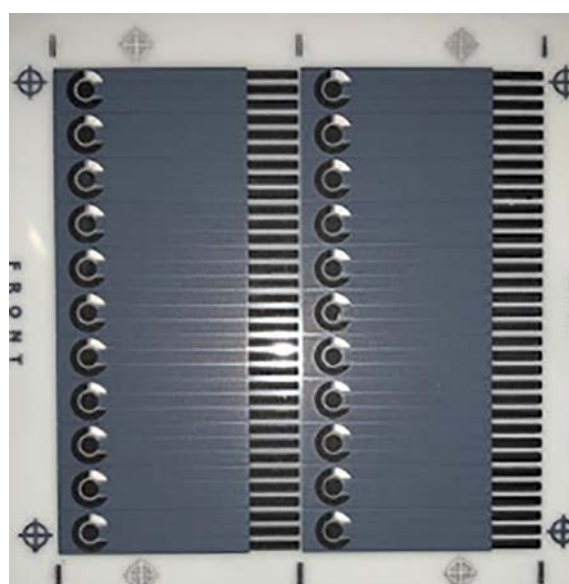
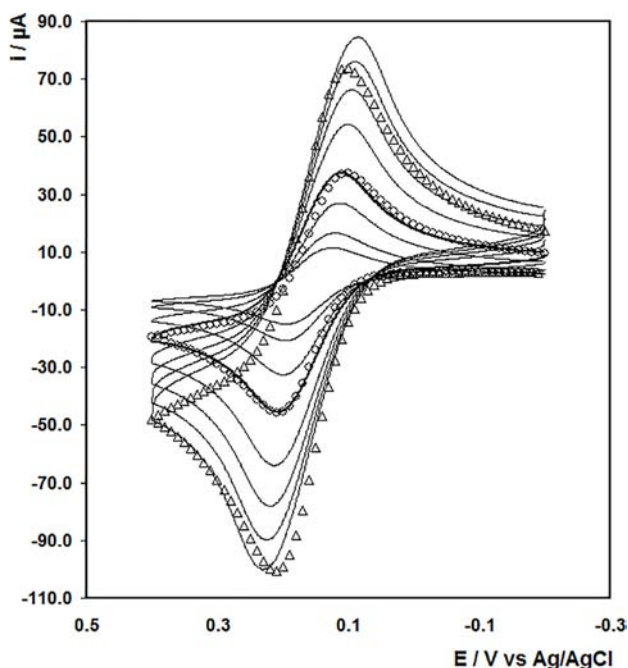


Figure 3.2. Screen-printed electrodes (22 individual sensor platforms are shown).



**Figure 3.3. Cyclic voltammograms of a 5 mM solution of ferrocene methanol at an SPy screen-printed electrode. The scan rates, from top to bottom, are 500, 400, 300, 100, 50, 40, 20 and 10  $\text{mV s}^{-1}$ . The open triangles and open circles are theoretical fits.**

separation at  $100 \text{ mV s}^{-1}$  is  $64 \text{ mV}$  and the ratio of the anodic ( $i_{pa}$ ) to cathodic ( $i_{pc}$ ) currents is  $1.01 \pm 0.08$ . This makes them excellent platforms for the development of sensors for pathogens or other contaminants within wastewater. Significantly, the capacitance current observed at potentials far from the faradaic peaks is very low, giving an excellent signal-to-noise ratio, in this case  $>40$ , which extends the concentration range over which detection can take place.

#### *Antibody selection and immobilisation*

Antibodies for the selective detection of Gram-positive and Gram-negative bacteria were sourced from Abcam, Cambridge Biosciences and HyTest, and their performance in assays for the detection of bacteria assessed. The HyTest antibodies performed best, based on their association constant with attenuated *E. coli*, and were therefore used in subsequent experiments.

Two strategies were pursued for the immobilisation of the antibodies: (1) the physisorption of the antibodies directly onto the screen-printed electrodes and (2) the

loading of antibodies within a polymer film. These strategies are described below:

1. **Physisorption of antibodies.** This approach would simplify ultimate mass manufacture. Initial attempts involved directly adsorbing the antibody from a  $100 \mu\text{M}$  solution onto the screen-printed electrode surface. This gave an antibody coverage of  $2.1 \pm 0.2 \times 10^{-12} \text{ mol cm}^{-2}$  ( $n=10$ ). The dynamic range is ultimately dictated by the number of binding sites on the sensor surface. This coverage, approximately 20% of a close-packed monolayer, was insufficient to allow the high bacteria concentration (untreated water) and the low concentration (post treatment) to be detected using a single sensor. The screen-printed electrode ink was reformulated to increase its hydrophobicity, with the objective of enabling the adsorption of more protein. This gave a higher antibody coverage, of  $6.8 \pm 0.3 \times 10^{-12} \text{ mol cm}^{-2}$ , but coverage remained too low to give a sufficiently wide, linear dynamic range.

2. **Antibodies loaded within a polymer film.** A second approach was investigated that allowed significantly more antibody to be deposited. This involved the deposition of a biomimetic polymer film on the electrode followed by the conjugation of the antibodies to the activated amide groups of the polymer. Figure 3.4 shows the *N*-isopropylacrylamide (NIPAM) polymer used to form drop-cast layers on the electrode. The key advantage of this strategy over monolayers is that a 3D film can be formed, allowing a greater total amount of antibody to be immobilised, extending the dynamic range and perhaps improving the limit of detection (LOD). Once the film is formed, the electrode is immersed in the antibody solution and conjugated. Figure 3.5 shows confocal fluorescence microscopy images of the *E. coli*

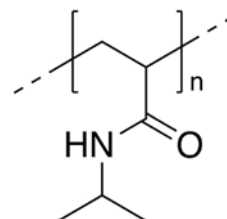


**Figure 3.4. Poly(NIPAM) polymer used for covalent attachment of pathogen antibodies in a 3D layer on electrodes.**

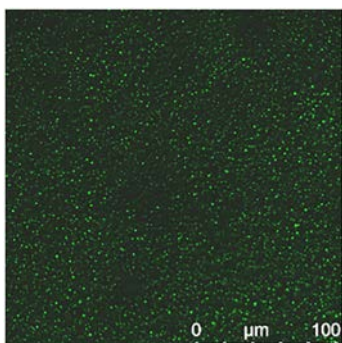


**Figure 3.5. Confocal fluorescence microscopy image of NIPAM polymer film deposited on an electrode following conjugation of FITC-labelled Gram-negative antibodies.**

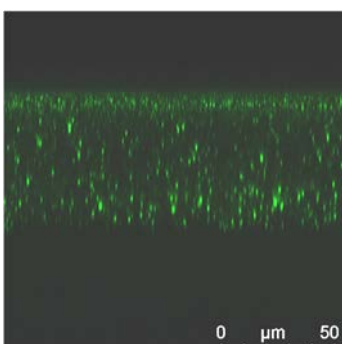


**Figure 3.6. Z-stack confocal fluorescence microscopy image of NIPAM polymer film deposited on an electrode following conjugation of FITC-labelled Gram-negative antibodies.**

antibodies labelled with the fluorescent dye fluorescein isothiocyanate (FITC). Significantly, emission is observed across the entire surface of the polymer film, suggesting a relatively uniform functionalisation of the antibodies. More significantly, Figure 3.6 shows a z-stack

image of the fluorescence through the film thickness, which indicates that the antibodies are distributed throughout the 50- $\mu\text{m}$ -thick polymer film. This demonstrates that the polymer is highly permeable, which maximises the number of pathogen-binding sites available, thus extending the upper limit of the calibration curve.

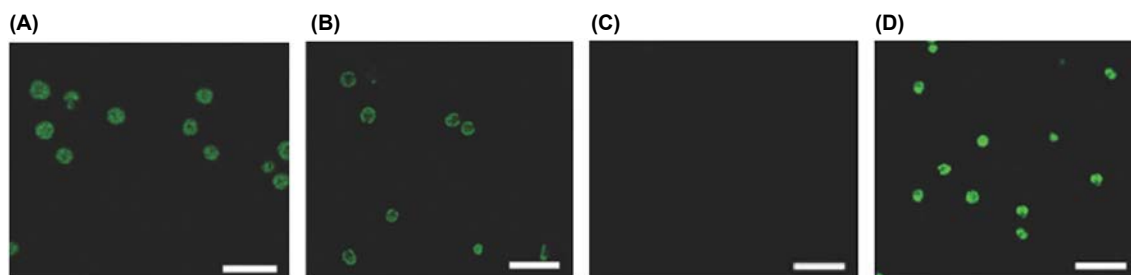
*Investigating the ability to regenerate the capture surface*

A second objective of Task 1.1 was to investigate the ability to regenerate the capture surface, so that it could be reused, by applying a voltage or flowing an electrolyte solution across it. Figure 3.7A shows *E. coli* captured on an electrode surface (open circuit) that had been functionalised with a film of an electronically conducting polymer, polypyrrole, that contains antibodies for *E. coli*. A comparison of Figure 3.7A and B shows that the number of captured bacteria decreases by approximately 25% when a potential of 0.5V is applied. However, applying 1.0V, which oxidises the polypyrrole film, triggers complete desorption of the captured bacteria (Figure 3.7C). Figure 3.7D shows that once the voltage is removed the *E. coli* can once again be captured on the antibody-functionalised electrode. This demonstrates achievement of our objective of enabling reversible bacteria binding using an electrical stimulus.

*Labels and sensors*

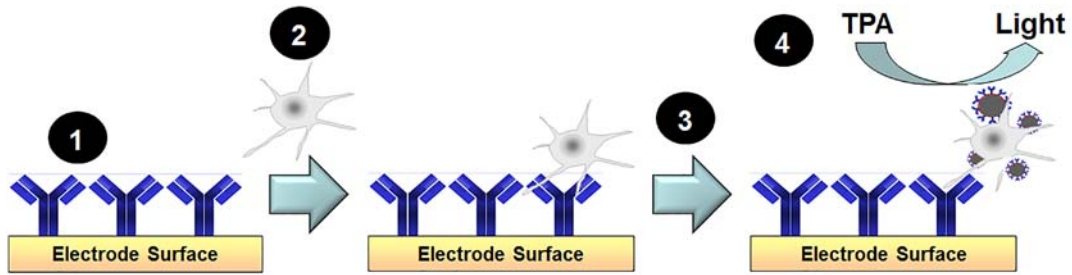
**Electrochemiluminescent pathogen sensors.**

Figure 3.8 illustrates the antibody sandwich assay with electrochemiluminescence (ECL) developed under the SPy programme for the detection and quantification



**Figure 3.7. (A) *E. coli* captured on a glassy carbon electrode functionalised with a 550 nm thick polypyrrole film containing capture antibodies for *E. coli*. (B) Captured *E. coli* when a voltage of 0.5V is applied. (C) Removal of captured *E. coli* when a voltage of +1.0V is applied so as to oxidise the polypyrrole film. (D) Rebinding of *E. coli* when the electrode is returned to open circuit.**





**Figure 3.8. Highly sensitive sensor for the detection and quantification of *E. coli* in water based on the generation of ECL when a voltage is applied. TPA, tripropylamide.**

of *E. coli*. The sensor comprises (1) electrodes whose surface is modified with immobilised antibodies for the selective capture of (2) *E. coli* from water samples, (3) detection antibodies modified with electrochemiluminescent dyes and (4) a co-reactant that, together with the dye, generates ECL, whose brightness depends on the concentration of *E. coli* present in the water sample.

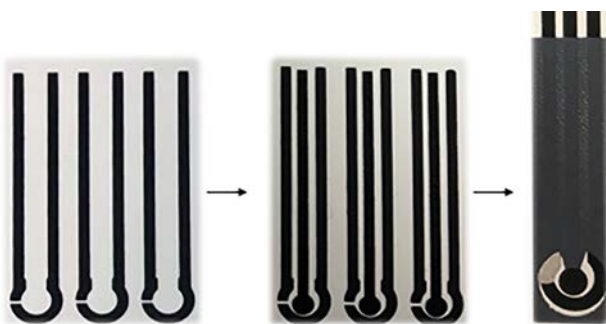
In the ECL assay, a dye (e.g. a ruthenium or copper complex) that becomes bound to the electrode surface in the presence of a target is oxidised by the application of an appropriate voltage to the electrode. In parallel, a co-reactant, such as tripropylamine, is also oxidised and when these two electrogenerated reagents meet light is emitted.

Figure 3.9 shows photographs of the sequentially printed reference, carbon counter and working electrodes that act as platforms for the creation of the antibody-based pathogen sensors shown in Figure 3.8. These electrodes were functionalised with capture

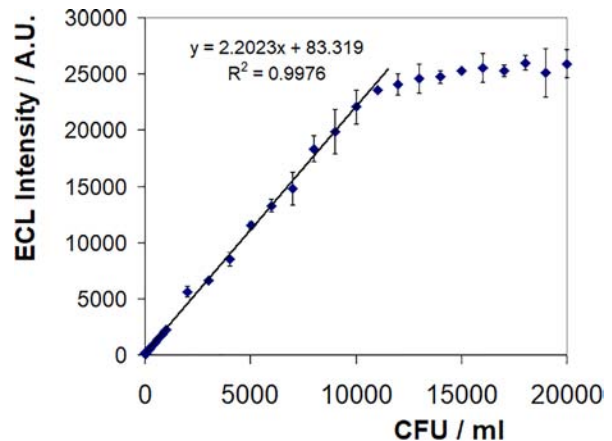
antibodies and used for the ECL-based detection of *E. coli*; the ECL dye used to label the detection antibody was a ruthenium metal complex.

As shown in Figure 3.10, once functionalised with capture antibodies, these sensors are capable of detecting *E. coli* across a wide dynamic range (approximately 40 to 10,000 colony-forming units (CFU) ml<sup>-1</sup>) with an LOD of 75 ± 6 CFU ml<sup>-1</sup>. This wide dynamic range and relatively low LOD make these sensors very suitable for monitoring pathogen levels within wastewater before treatment. However, for applications where the objective is to purify the water to a level that is suitable for drinking or washing food produce, a lower LOD is needed. According to the WHO, a zero count of *E. coli* per 100 ml of water is considered safe for drinking, while a most probable number count of 1–10 per 100 ml is regarded low risk.

The intensity of the light depends on the number of molecules within the label and can range from one to several thousand in the case of a nanoparticle label. Therefore, part of the programme focused on



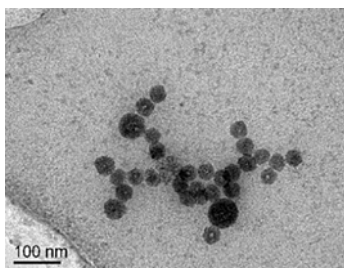
**Figure 3.9. Integrated sensor platform that incorporates an Ag/AgCl reference electrode as well as carbon counter and working electrodes. This design allows the sensor to simply be inserted into the wastewater sample without the need for additional electrodes to be added.**



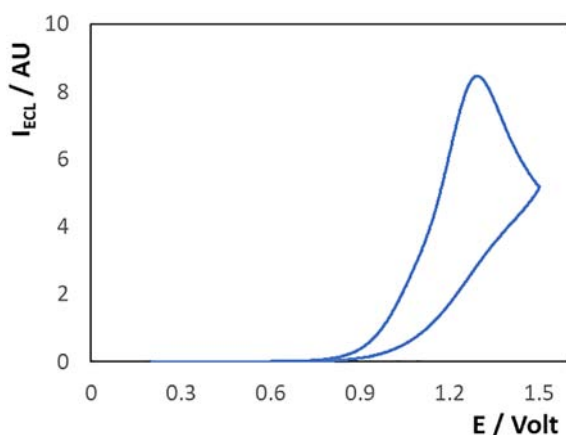
**Figure 3.10. Dependence of the ECL intensity on the concentration of *E. coli* in a water sample.**

developing high-brightness, electrochemiluminescent nanoparticles as labels for the detection antibodies.

As illustrated in Figure 3.11, working in close collaboration with Professor Yann Pellegrin in Nantes, France, we synthesised and characterised the ECL generated by silicate nanoparticles loaded with ruthenium and copper complexes. The switch to copper is important in terms of its dramatically lower cost and toxicity. Significantly, these particles are stable even in food and pharmaceutical wastewaters, since the long-standing barrier of ligand loss/exchange from the copper complex has been prevented through the novel encapsulation/nanoparticle formation process. Figure 3.12 shows that the ruthenium-loaded nanoparticles generate light (ECL), with the maximum brightness occurring at +1.31 V. Significantly, the particle brightness is approximately 400-fold higher than that observed for a single metal complex, allowing targets such as pathogens and priority pollutants to be detected at lower concentrations.



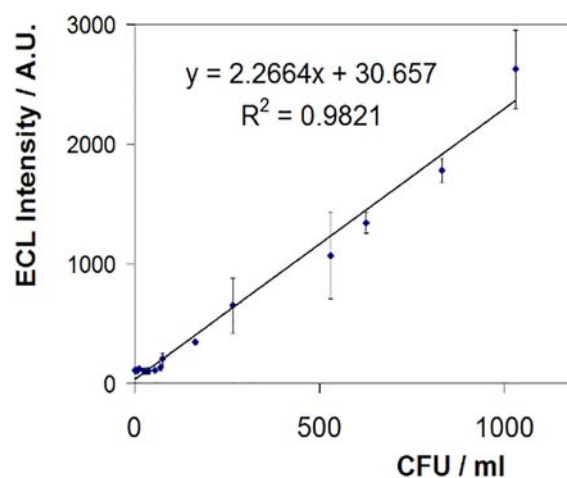
**Figure 3.11. High-brightness silicate nanoparticles loaded with ruthenium complexes.**



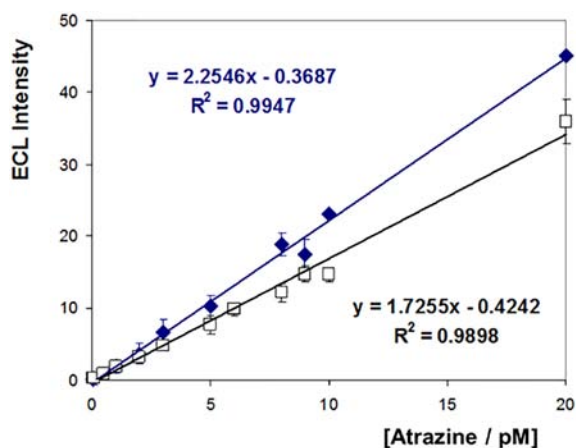
**Figure 3.12. ECL from a 1 μM suspension of silicate nanoparticles loaded with a ruthenium poly-pyridyl complex.**

Figure 3.13 shows the dependence of the ECL intensity on the *E. coli* concentration (in CFU ml<sup>-1</sup>). It shows that the sensor response depends linearly on CFU ml<sup>-1</sup> from approximately 60 CFU ml<sup>-1</sup> to approximately 800 CFU ml<sup>-1</sup> with an LOD of approximately 43 ± 6 CFU ml<sup>-1</sup>. Significantly, by using a polyethylene glycol layer, which prevents the non-specific binding of proteins within the sample and blocks access to the binding sites, the sensor maintains its calibration slope to within 92 ± 3% of its clean buffer value when tested in wastewater from a food production facility in France. These results demonstrate that *E. coli* can be detected at relatively low concentrations (CFU ml<sup>-1</sup>) in complex wastewater samples using this approach.

**ECL-based immunoassay for the detection of priority pollutants.** The antibody sandwich assay format illustrated in Figure 3.8 was used for the detection of atrazine, a chlorinated triazine systemic herbicide that is used to selectively control annual grasses and broadleaf weeds before they emerge. As illustrated in Figure 3.14, a highly sensitive ECL-based immunoassay for the detection of atrazine has been developed. A mercaptoundecanoic acid monolayer was used in conjunction with 1-ethyl-3-(3-dimethylaminopropyl)carbodiimide coupling to immobilise the primary atrazine antibody onto a gold electrode in a way that preserves its bioactivity. The detection antibody was functionalised with an amino-functionalised ruthenium complex (Pellegrin, Nantes), again using EDC coupling. In a antibody sandwich assay, as shown in Figure 3.14, the intensity of the light emitted at 610 nm increases linearly with an



**Figure 3.13. Dependence of the ECL intensity on the concentration of *E. coli* in a water sample.**



**Figure 3.14.** Dependence of the ECL light intensity on the concentration of atrazine in an antibody sandwich assay. The detection antibody is labelled with the ECL-active ruthenium complex. Blue shows data for freshwater and black shows data for salt water.

increasing concentration of atrazine. Significantly, by developing an immobilisation strategy that preserves the activity of the capture antibody in combination with the novel high-brightness ruthenium label, sub-picomolar concentrations (comparable to a single grain of salt in an Olympic swimming pool of pure water) of the herbicide can be detected. Moreover, the immobilisation approach maintains the capture antibody in a biomimetic environment, allowing the assay to be performed in salt water with only a modest loss (approximately 25%) of analytical sensitivity.

**Stability of sensors within the reactor.** SPy technology, for the destruction of recalcitrant organic materials, produces highly reactive hydroxyl radicals that are capable of easily destroying the immobilised antibodies used to detect target analytes, such as pathogenic bacteria. Figure 3.15 shows the relationship between the concentration of bacteria in the reactor measured using our ECL-based pathogen sensor with samples collected from the reactor and analysed *ex situ* and the concentration measured by operating the sensor inside the reactor. The ideal relationship would be a direct, unbiased correlation (with the slope and correlation coefficient both equal to 1, and an intercept of zero). However, Figure 3.15 shows that the results do not correlate (correlation coefficient,  $R^2$ , of 0.65). This is because the performance of the sensor quickly fails when exposed to hydroxyl radicals within the reactor

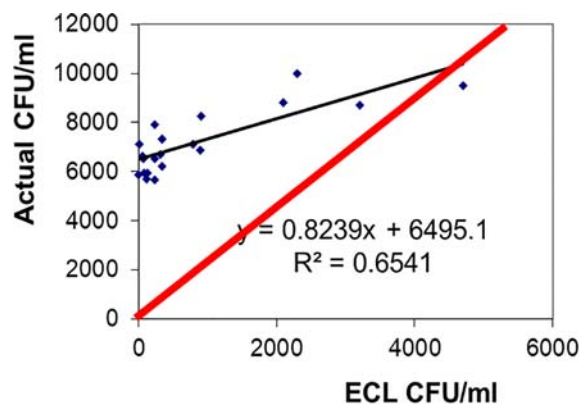


**Figure 3.15.** Relationship between the pathogen concentration measured using sampling and *ex situ* analysis ( $y$ -axis) and that determined when the sensor is placed inside the reactor. Blue dots indicate experimental data (the black line is the best fit regression line with the equation provided) collected using the ECL sensor within the reactor. The red line shows the behaviour expected for a direct, unbiased correlation. In both cases, the pathogen concentration has been measured using the SPy ECL-based pathogen sensor. The *in situ* data were collected as the reactor was actively producing hydroxyl radicals.

(half-life of approximately 20 s) due to the degradation of the sensor materials. Therefore, our data strongly suggest that using UV-Vis spectroscopy to monitor the decolourisation and decomposition of the organic pollutants is the best way forward in monitoring the destruction of the recalcitrant organic compounds.

### 3.1.2 Task 1.2: establishing a UV-Vis method for the estimation of the total organic carbon content of wastewater and processed water streams

The objective of Task 1.2 was to develop a UV-Vis spectroscopy method that could be used within the reactor as a cost-effective, real-time approach to monitoring effective TOC content to minimise the treatment time.

#### Ex situ monitoring

Figure 3.16 shows the changes that occur in the UV-Vis absorbance spectrum of a gemcitabine (a chemotherapeutic drug used to treat bladder and breast cancers) solution following SPy treatment



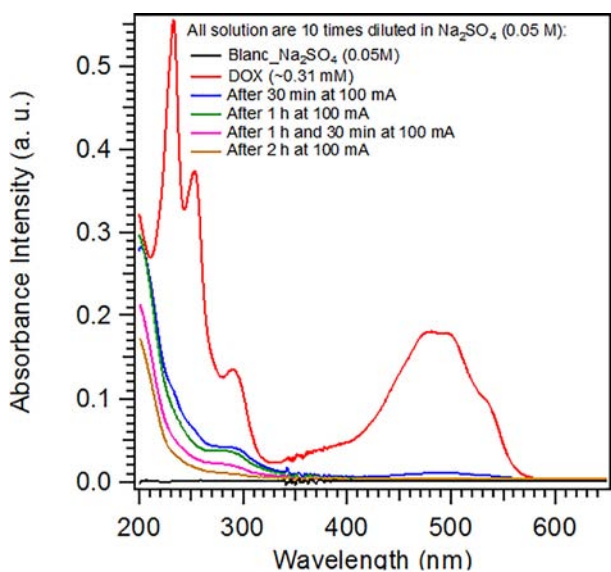


**Figure 3.16.** UV-Vis spectra of the blank electrolyte solution (Blanc\_Na<sub>2</sub>SO<sub>4</sub>) and the parent drug doxorubicin (DOX), and after degradation using electrogenerated hydroxyl radicals for 30, 60, 90 and 120 minutes.

at a current density of 100 mA for defined periods of time. In these experiments, the contents of the reactor were periodically sampled and transferred to a cuvette for measurement. Significantly, these data confirm successful decomposition of the target within a relatively short period of time and show that UV-Vis spectroscopy can be used outside the reactor to monitor the decomposition of APIs. To investigate the generality of the approach, the decomposition of other drugs was investigated, and UV-Vis spectroscopy was able to detect gemcitabine at a concentration of 90 μM, while doxorubicin was detected at 30 μM.

#### In situ monitoring

The ability to monitor the decomposition of organic materials using *in situ* UV-Vis spectroscopy within the reactor was accomplished by incorporating two 12-mm-diameter, 1.5-mm-thick, UV-Vis-coated, double-convex lenses into the two opposing side walls of the reactor. This allows excitation-wavelength light to enter the reactor, be absorbed by any organic materials that have not been mineralised at wavelengths between 250 and 700 nm, exit the reactor and be detected by the spectrometer. The lens is somewhat larger than the 10-mm-diameter probe beam of the spectrometer, facilitating alignment with the entrance slit. Figure 3.17 shows that this “through

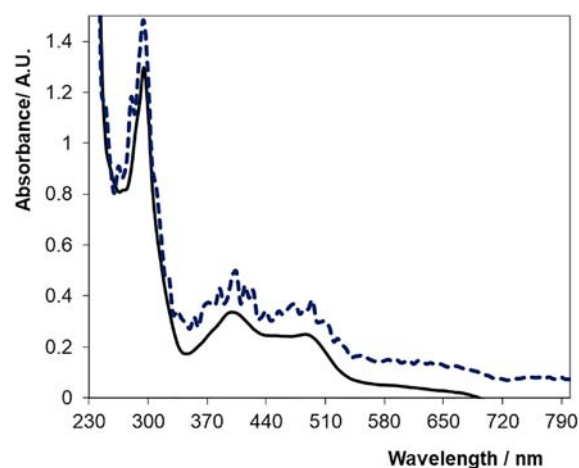


**Figure 3.17.** UV-Vis spectra of a pharma wastewater stream in the SPy reactor. The solid black line shows the spectrum in the absence of BDD particles, while the dashed blue line (offset by 0.2 absorbance units for clarity) is the spectrum obtained when BDD particles are present. The noise is caused by scattering of the BDD particles.

reactor” configuration is effective and produces high-quality spectra. In the presence of the BDD particles, significant noise due to scattering is observed, but the spectral features remain clearly visible, and the absorbance values correlate with the concentration of coloured species in the wastewater.

#### Correlation between UV-Vis spectroscopy and TOC

Figure 3.18 shows the correlation between the concentration of gemcitabine determined using UV-Vis spectroscopy and the concentration found

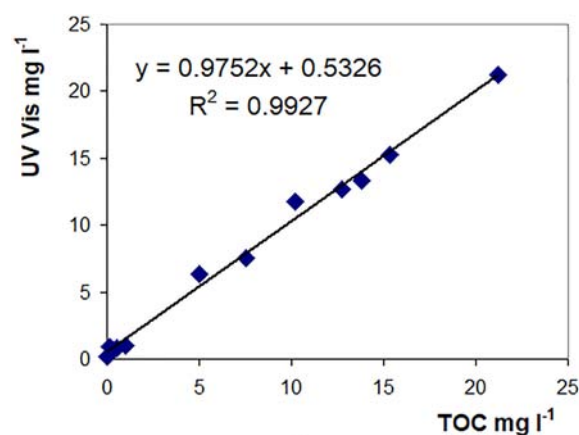


**Figure 3.18.** Correlation of gemcitabine concentration as determined using UV-Vis spectroscopy with traditional TOC measurement.

using a traditional method for measuring TOC content for a range of gemcitabine concentrations. Ideally, a slope of unity and an intercept of zero would be observed in this correlation plot. The experimental slope,  $0.975 \pm 0.067$ , is indistinguishable from a slope indicating unity, suggesting a direct correlation between the concentrations determined using UV-Vis spectroscopy and the traditional method for measuring TOC content. The intercept,  $0.532 \pm 0.115$ , indicates that the UV-Vis approach tends to slightly overestimate the concentration of the drug in solution, i.e. there is some systematic bias, but this can be calibrated for. The lower limit above which the correlation is observed is approximately  $10 \mu\text{M}$ , making the low-cost UV-Vis approach sufficiently sensitive for monitoring treatment of a broad range of pharmaceutical wastewaters.

### 3.2 Work Package 2: Optimised Particles for Wastewater Treatment

#### 3.2.1 Task 2.1: modelling of electric field distribution

The potential distribution between drive electrodes was modelled using COMSOL Multiphysics software to identify the optimal conditions (especially electrode size and placement, conducting diamond particle size and composition/conductivity) for optimised hydroxyl radical generation and minimised energy costs.

##### *Hydroxyl radical concentrations around boron-doped diamond particles*

The hydroxyl radical concentration profiles around the particles were successfully modelled to identify the optimum concentration of particles in suspension relative to the concentration of the organic pollutant. For example, Figure 3.19 shows hydroxyl radical concentration as a function of distance from the particle surface, where the contaminant concentration varies from 1.0 M to 0.25 M. This range is intended to encompass the concentrations of organic contaminants found in first- and second-wash wastewaters from a food production facility. This modelling indicates that, even when the pollutant concentration is low, there are essentially no hydroxyl radicals further than about 25 nm from the particle surface. This is because the radical lifetime is short ( $2\text{--}5 \mu\text{s}$ ) and confirms the absolute need to generate

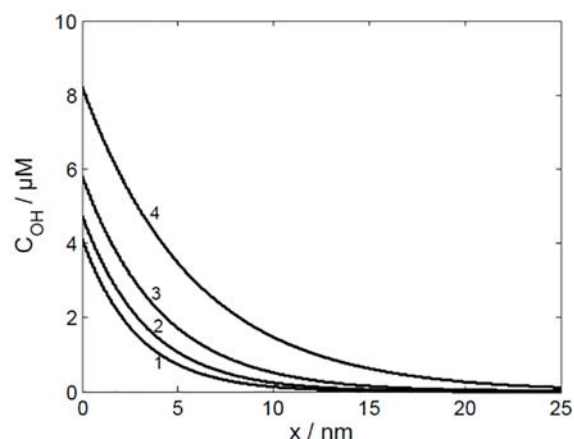


**Figure 3.19. Calculated concentration–distance profiles of hydroxyl radicals during oxidation of (1) 1.0 M, (2) 0.75 M, (3) 0.5 M and (4) 0.25 M gemcitabine. The diffusion coefficient of the hydroxyl radicals is  $2.2 \times 10^5 \text{ cm}^2 \text{ s}^{-1}$  and the rate of drug oxidation is  $1.3 \times 10^3 \text{ M}^{-1} \text{ s}^{-1}$ .  $C_{\text{OH}}$ , hydroxyl radical concentration;  $x$ , distance.**

hydroxyl radicals throughout the entire volume of the wastewater sample and not just at the surface of a single electrode, as has been reported previously in the literature. With this information, and knowledge about the potentials required to generate hydroxyl radicals from Work Package (WP) 1, the potential distribution between drive electrodes located within the reactor was modelled to optimise reactor efficiency.

##### *COMSOL Multiphysics modelling of electric field distribution in reactor*

The electric field distribution that drives the voltage generated within the BDD particles, leading to hydroxyl radical production, was modelled using COMSOL Multiphysics software. This is a computer-based simulation platform that encompasses all of the steps in the modelling workflow. It allows geometries, material properties and other key parameters, such as the electric field strength, to be defined and then the model is built and the effects of changing parameters can be visualised. As illustrated in Figure 3.20, an *in silico* model of the experimental cell has been developed. This model correctly predicts a more intense electric field close to the feeder electrodes, which we observed experimentally. The predicted electric field distribution through the solution was used to inform the selection of the optimum BDD particle size and the positioning of the feeder electrodes.

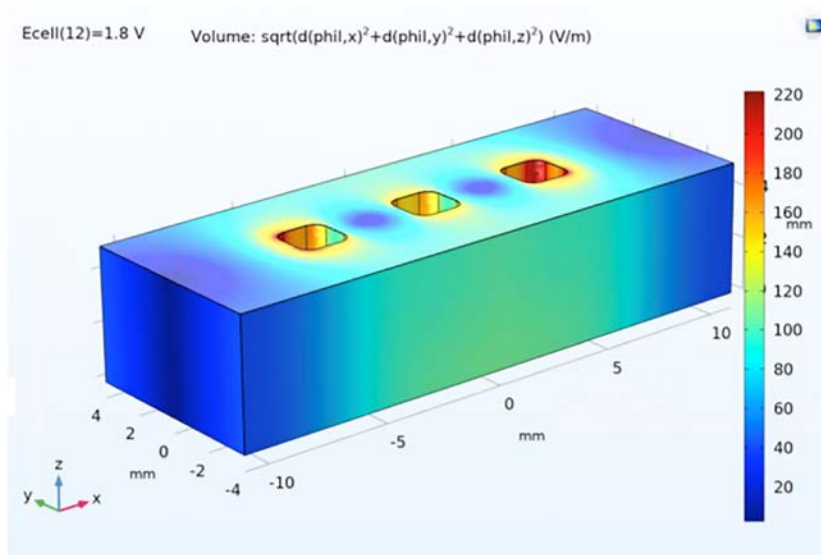


**Figure 3.20.** Prediction of the electric field distribution through solution using COMSOL Multiphysics software.

### 3.2.2 Task 2.2: optimising particles for wireless wastewater treatment

The objective of Task 2.2 was to identify the optimum source of BDD particles for use in the reactor. BDD electrodes and particles ( $50 \leq \text{diameter} \leq 2000 \mu\text{m}$ ) were sourced from Hunan Boromond, Ultra-Hard Materials, Element Six and CEA France. These materials were fully characterised using electrochemistry and Raman microscopy and based on their ability to generate hydroxyl radicals. This revealed that both the boron doping level and surface termination play key roles in dictating the efficiency of hydroxyl radical production. Specifically, surface termination using hydrogen is significantly better than using traditional oxide.

#### *Impact of boron doping level*

The optimisation of boron loading within the BDD material for the simultaneous production of hydroxyl radicals (inner sphere electron transfer reaction) was investigated. Two different doping levels were considered:  $5 \times 10^{20} \text{ atoms cm}^{-3}$  and  $2 \times 10^{21} \text{ atoms cm}^{-3}$ . As shown in Figure 3.21, the electrogenerated hydroxyl radicals are used to convert coumarin into 7-hydroxycoumarin (7OHC), which can be detected using fluorescence.

Cyclic voltammetry was used to investigate the hydroxyl radical-generating ability of the two materials and the results obtained are shown in Figure 3.22.

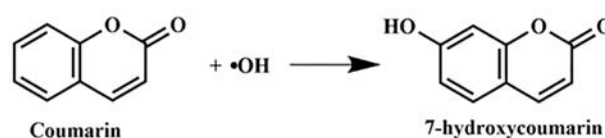


**Figure 3.21.** Formation of fluorescent 7OHC from coumarin using electrogenerated hydroxyl radicals.

The potentials at which hydroxyl radicals are produced are similar for the two materials. However, despite the relatively small difference in boron loading, the rate of electron transfer to electroactive species undergoing outer sphere electron transfer is significantly higher for the higher boron loading. The heterogeneous electron transfer rate constant  $k^0$  between ferrocene methanol in solution and the BDD material was calculated to be  $0.11 \times 10^{-2} \text{ cm s}^{-1}$  and  $0.34 \times 10^{-2} \text{ cm s}^{-1}$  for the BDD material with lowest and highest boron loading, respectively. The more highly doped BDD material allows coumarin and 7OHC to be electrochemically detected at a concentration of  $10 \mu\text{M}$ . This electrode BDD material opens up the possibility of using the same electrode, operating at different potentials, both to produce hydroxyl radicals and to monitor the concentration of electroactive species in solution. Fluorescence, UV-Vis spectroscopy and square wave voltammetry (SWV) measurements show that the 7OHC is the dominant product, but that there

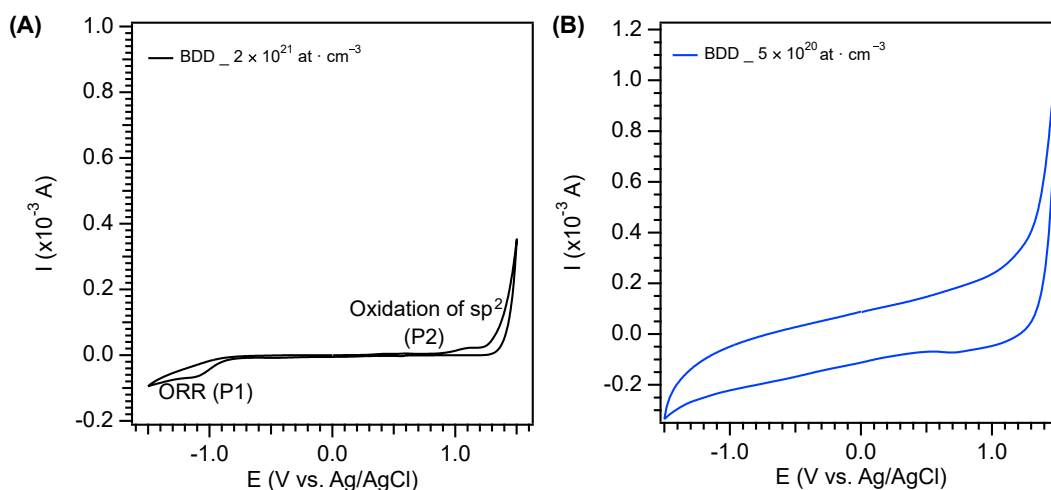
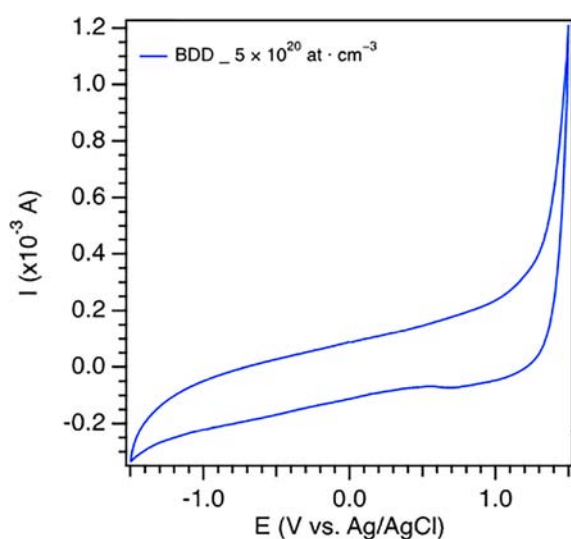


**Figure 3.22.** Cyclic voltammograms of BDD materials with boron concentrations of (A)  $2 \times 10^{21}$  atoms  $\text{cm}^{-3}$  and (B)  $5 \times 10^{20}$  atoms  $\text{cm}^{-3}$ . The scan rate was  $50 \text{ mVs}^{-1}$  and the electrolyte used was  $0.5 \text{ M KCl}$ .

is a minor side-product, most likely a hydroxylated polymer. The ratio of 7OHC to this side-product can be influenced by the nature of the BDD electrode and the potential waveform, allowing the extent of electrode coating and passivation to be minimised.

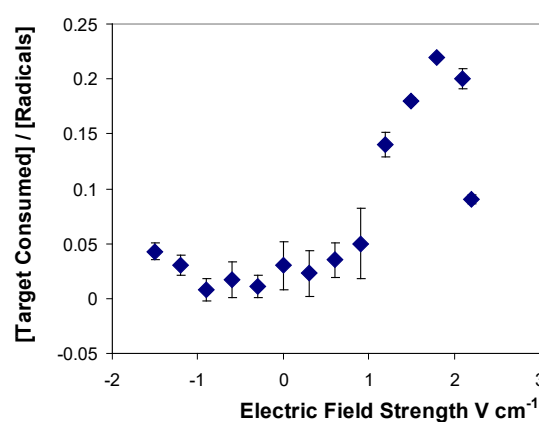
#### *Rate of hydroxyl radical production*

Figure 3.23 shows the response in terms of current when the potential of BDD is scanned from  $-1.500$  to  $+1.500 \text{ V}$ . The large current observed at potentials more positive than approximately  $+1.2 \text{ V}$  represents the



**Figure 3.23.** Cyclic voltammograms of BDD electrodes with a boron concentration of  $5 \times 10^{20}$  atoms  $\text{cm}^{-3}$ . The scan rate was  $50 \text{ mVs}^{-1}$  and the electrolyte used was  $0.5 \text{ M KCl}$ .

production of hydroxyl radicals, and their concentration can be determined by measuring the charge passed as a function of the applied potential. The fraction of these radicals that goes on to decompose the target pharmaceutical, e.g. the anti-cancer drug adriamycin, was measured using UV-Vis spectroscopy and high-performance liquid chromatography (HPLC). The ratio between the two rates (hydroxyl radical production to target decomposition) was used to identify the optimum conditions for wastewater treatment using a suspension of BDD within an electric field. Figure 3.24 shows how varying the voltage affects the ratio of the concentration of radicals produced to the concentration of the target decomposed. Irrespective of the electric field strength (voltage), only a fraction of the radicals



**Figure 3.24.** Ratio of the concentrations of adriamycin decomposed to the radical produced as a function of the voltage. The electrolyte used was  $0.5 \text{ M KCl}$ .



produced actually decompose the organic pollutant. This is because the lifetime of the radical is short ( $5\ \mu\text{s}$ ) and, unless the concentration of the organic materials is very high, the probability of the radical and organic molecule colliding is relatively low. In this sense, the system has a significant excess of the chemical that decomposes the organic materials, making it tolerant to unexpected increases in the TOC content of the incoming wastewater.

### 3.3 Work Package 3: Integrated Reactor

#### 3.3.1 Task 3.1: reactor design

Task 3.1 focused on creating a prototype reactor capable of processing wastewater at  $1\text{--}10\ \text{litre h}^{-1}$ . Models of a prototype reactor were created using finite element simulations (with COMSOL Multiphysics software) to describe the flow dynamics and electric field distribution. Fluid flow modelling of the wastewater loaded with BDD particles is shown in Figure 3.25, where the wastewater contained  $9.25 \times 10^{-4}\ \text{M}$  gemcitabine. This figure shows the flow of the solution entering the reactor at maximum velocity ( $100\ \text{cm s}^{-1}$ ), which is represented by red vector arrows. Once the solution entered the reactor, the velocity decreased to below  $10\ \text{cm s}^{-1}$  and the flow pattern changed from laminar to turbulent. This is an intrinsic part of our reactor design and ensures thorough mixing of the wastewater stream and the BDD particles that drive the AOP.

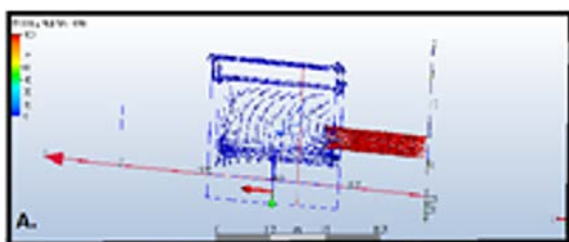


**Figure 3.25. Flow of wastewater stream through the SPy reactor. The entrance is to the right-hand side. The red vectors indicate a high flow rate (laminar flow), while the blue vectors indicate a lower velocity and show turbulent flow intended to drive complete mixing of the incoming wastewater and the BDD particles as well as to help keep the particles in suspension.**

Informed by the flow modelling, computer-aided designs (CADs) were generated, such as those illustrated in Figures 3.26 and 3.27. To enable 3D printing, the CAD file was first converted to standard tessellation format (.stl). The .stl file was uploaded to the 3D printer (UltiMaker 5), which was calibrated (extruders and printing base) to improve the accuracy of printing. The infill density used was 30% to ensure that the reactor had sufficient mechanical strength while minimising the cost of materials. The reactor itself was printed using a range of materials, including polylactic acid (PLA), acrylonitrile butadiene styrene (ABS) and polyethylene terephthalate glycol-modified (PETG), which has better mechanical and chemical stability than ABS. Supports were printed using water-soluble poly-vinyl alcohol. The type of reactor shown in Figure 3.26 takes 68 hours to print.

The design shown in Figure 3.26 with a single pair of feeder electrodes is robust, easy to operate and flexible in cases of fluctuating wastewater streams, and avoids the requirement for the multiple electrical connections that are needed for electrodes wired in series. The core design of this flow-through reactor, with a volume of  $100\ \text{cm}^3$ , was used extensively to investigate the ability to generate hydroxyl radicals wirelessly using BDD particles, and, by changing the design to alter the composition, size, separation and relative position of the feeder electrodes, to correlate real-world performance with that predicted by the modelling. It was also used to test wastewater samples from a Dublin-based pharmaceutical company and a food processing plant, from where samples were shipped overnight and then treated at Dublin City University (DCU). Significantly, key predictions of the analytical and COMSOL Multiphysics modelling, such as the effect of the electrode separation, the electric field strength and the particle size, generally correlate very strongly with the experimental data obtained in low-concentration ( $<0.1\ \text{M}$ ) electrolytes or when electrolyte is not deliberately added. The predictions of these two models correlate well with the potential-dependent behaviour shown in Figure 3.19, i.e. the rate of pharmaceutical decomposition initially increasing with increasing voltage (electric field strength) before decreasing as a result of water oxidation dominating the response at more positive potentials.

However, in more conducting solutions (electrolyte concentration  $>0.2\ \text{M}$ ) or in solutions with a high

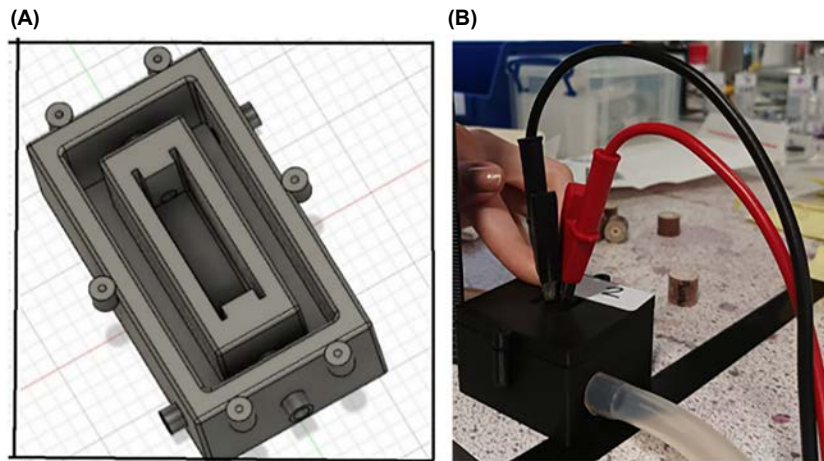


**Figure 3.26. (A) SPy reactor featuring a pair of feeder electrodes. (B) Photograph of reactor that was 3D printed using PETG.**

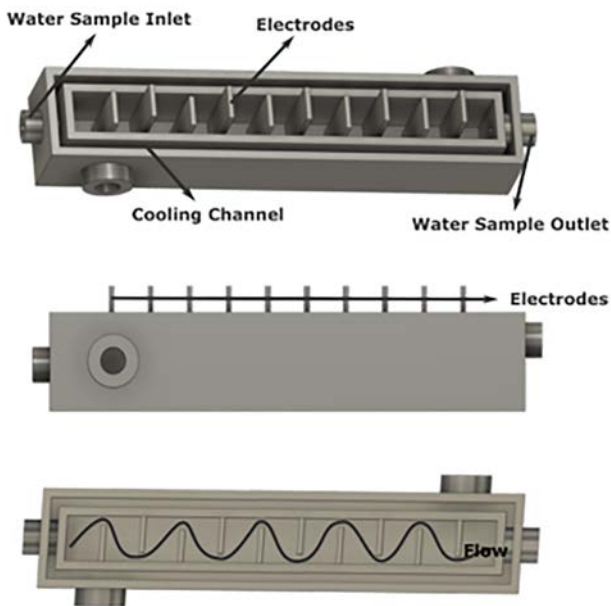


**Figure 3.27. Schematic of flow-through reactor for wireless treatment of wastewater.**

concentration of organic material that can ionise, e.g. naturally occurring (poly) acids in food waste, the electric field strength is significantly reduced and joule heating due to the passage of an electric current through the sample causes deviations as a result of enhanced mass transport. The challenges encountered during the processing of food-related wastewater are presented under WP4.

Multi-electrode systems were also developed. The key advantage of these systems is that electrode separation can be made sufficiently short such that the voltage that must be applied to the feeder electrodes

can be sufficiently low to extend their lifetime. For example, for 1 mm BDD particles a field strength of  $50 \text{ V cm}^{-1}$  is required to achieve a sufficiently positive voltage at the anodic pole of the particle to produce hydroxyl radicals. The titanium electrodes are stable at potentials up to 100 V, so a separation of up to 2 cm between feeder electrodes can be used. Thus, for the maximum titanium electrode size available,  $10 \text{ cm} \times 10 \text{ cm}$ , the cell volume would be  $10 \text{ cm} \times 10 \text{ cm} \times 2 \text{ cm}$  or  $200 \text{ cm}^3$ , provided that the electrolyte concentration is sufficiently low, e.g. as found in pharmaceutical wastewater. If the separation distance between feeder electrodes is increased to enable an increase in sample volume, the voltage applied to the feeder electrodes must also be increased. This would reduce their lifetime from hundreds of hours to less than 5 hours, because of corrosion, even if they are protected by an optimised oxide coating. One solution that enables the sample volume to be increased without the need to apply a high voltage, as shown in Figure 3.27, is to use several pairs of feeder electrodes. This enables the separation distance between electrodes to be kept short, meaning that the voltage that must be applied to the feeder electrodes can be sufficiently low to give them a long operational lifetime. Moreover, by optimising the arrangement of feeder electrodes, the flow path can be optimised to encourage mixing and to maintain the BDD particles in suspension. However, multi-electrode systems are more difficult to produce, use a greater quantity of titanium and take significantly longer to set up than systems with a single pair of electrodes. Moreover, routine maintenance of multi-electrode

systems is more time-consuming, which was identified as a barrier to successful deployment by our industry partners.

### **3.3.2 Task 3.2: reactor fabrication**

The objective of Task 3.2 was to rapidly produce small (1–10 litre per hour flow-through) prototype reactors using 3D printing techniques, initially using ABS.

#### *3D printing*

The CAD file used to design and model the SPy reactor was converted to a .stl format and was printed using an UltiMaker 5 3D printer. The .stl file was uploaded to the printer, which was calibrated (extruders and printing base) to improve the accuracy of printing. The infill density used varied from 20% to 50% to ensure that the reactor had sufficient mechanical strength while minimising the cost of materials and printing time. The performance of a variety of filament materials, i.e. PLA, ABS and PETG, which have better mechanical and chemical stability than ABS, was investigated. Supports were printed using water-soluble poly-vinyl alcohol. This is quite a time-consuming process, and the reactor shown in Figure 3.27 took 68 hours to print.

#### *Stability of 3D filament under wastewater treatment conditions*

Initial designs of the reactors printed using ABS rapidly showed signs of decomposition, e.g. a decrease in surface colour of 30% within 2 hours, when used to treat wastewater samples. Moreover, Charpy impact tests indicate that cracks form after just 4 hours' exposure. One approach investigated to address this issue was the use of a more robust material, namely PETG, that is chemically more stable. Reactors printed using PETG proved very stable when operated for periods of up to 50 hours. However, modelling indicated that the feeder electrodes themselves generate significant concentrations of hydroxyl radicals. In the initial designs, the feeder electrodes were touching the reactor side walls, allowing the hydroxyl radicals generated to attack the reactor walls, causing premature failure. This issue was exacerbated by the use of square corners that acted as stress risers. A simple solution that allows ABS to be used while giving a reactor lifetime of > 100 hours

is to position the feeder electrodes far enough from the walls such that the time required for the hydroxyl radicals to diffuse to the walls is longer than their lifetime ( $\approx 5 \mu\text{s}$ ), meaning that they decompose in solution before they can attack the reactor walls.

#### *Aluminium or titanium feeder electrodes*

Intense electric fields, i.e. 50 to 100 V cm<sup>-1</sup>, are required for small BDD particles. This means that even if feeder electrodes are separated by only 1 cm (which is important, since this in part dictates the reactor volume) voltages of the order of 50–100 V must be applied to the feeder electrodes. These high voltages pose significant challenges in terms of the stability of the feeder electrodes used to generate the electric field in the wastewater sample. Therefore, the stability of aluminium and titanium feeder electrodes was investigated. The electrodes were weighed and measured (in dimensions x, y and z) before the experiments. Two feeder electrodes were then placed in the reactor shown in Figure 3.26, which was filled with Milli-Q water without any added organic pollutant. A voltage was then applied, and the weight and physical size of the electrodes measured periodically, typically every 30 minutes. A stable electrode was defined as one that lost less than 5% of its weight and that changed less than 10% in any one of the dimensions (x, y or z). The findings of this analysis are outlined below:

- **Aluminium.** Oxide-coated aluminium is stable for periods up to only 1.5 hours at 50 V. Decreasing the applied voltage to 30 V, which could be used with larger BDD particles, extended the lifetime to 5 hours. Aluminium coated with a silicone resin extended the lifetime to 20 ± 7 hours. However, as reflected by the large error bar, the coating process was not very reproducible, with the silicone coating delaminating from the aluminium substrate. None of these lifetimes is sufficient for meaningful real-world applications and so titanium was investigated.
- **Titanium.** Titanium forms an oxide upon exposure to air, i.e. a native oxide, but an oxide layer can also be grown electrochemically. By applying positive potentials of +1.5 V, oxide layers of controlled density and thickness can be created. These oxide layers can provide substantial protection from corrosion at the positive potentials

required for the wireless treatment of wastewater. The effects of applying oxidation potentials of between +1.5V and 2.0V for periods of between 30 seconds and 20 minutes on the stability of the electrodes when used for wastewater treatment were investigated. Figure 3.28 shows the effect of applying 1.8V for 120 s to a titanium electrode. The change in colour reflects the formation of the oxide layer, and its colour depends on the conditions used for deposition. Significantly, titanium electrodes oxidised at +2V for 300 s were the most stable towards oxidative corrosion. Specifically, when oxidised at 1.8V for 300 s, the electrodes are stable at voltages up to 100V for periods of at least 30 hours. The combination of the applied voltage (controls rate of oxide formation) and time (controls oxide thickness) is important in controlling the performance of the feeder electrodes.

#### *Carbon-based screen-printed feeder electrodes*

The use of screen-printed electrodes as feeder electrodes in the SPy prototype reactor would have several advantages over metal-based electrodes, including lower costs, mechanical flexibility and the ability to make them into arbitrary sizes (up to 1 m × 1 m) and shapes. Therefore, a range of novel, hydrophobic and chemically stable inks were formulated. Table 3.1 shows the range of compositions investigated with a view to creating electrodes that would be stable at potentials of 100V or higher and



**Figure 3.28.** Upper electrode is a pristine titanium electrode and the lower electrode is a titanium electrode following oxidation at +1.8V for 300 s.

**Table 3.1. Composition of the ink used to screen-print electrodes to act as feeder electrodes in the SPy prototype reactor**

Ink component	Weight (%)
E15/45 M	5–12
Cyrene	25–35
Propylene glycol methyl ether acetate (PGMEA)	20–30
Plasticiser – DBE 9	1–5
Graphite	15–25
Carbon	10–15

whose use would avoid significant gas evolution, which tends to cause delamination from the support.

These electrodes had a lifetime of 6 hours for wastewater treatment at a voltage of 50V. The dominant cause of failure was failure of the seal between the screen-printed coating and the underlying substrate, e.g. aluminium in the electrode shown in Figure 3.29. This allowed the solution to come into contact with the aluminium substrate, which then rapidly corroded. In this sense, the issue is with the coating quality, i.e. the continuity of the layer at the edges, not the carbon-based ink formulation.

#### *Boron-doped diamond feeder electrodes*

Making the feeder electrodes out of the same material as the particles that generate the hydroxyl radicals, i.e. BDD, would avoid any issue with electrochemical stability and corrosion. BDD particles are stable at 100V for periods of time up to at least 50 hours



**Figure 3.29.** Photograph of the screen-printed carbon-based electrode tested as a feeder electrode in the SPy reactor.



(limit of testing), with no evidence of decomposition or corrosion. However, the cost (approximately €50–70 per cm<sup>2</sup>) would be a significant barrier to scaling up.

WP3 was completed successfully, with all of the deliverables and milestones being realised. The oxide-coated titanium electrodes, coupled with 2 mm BDD particles, gives a projected operational lifetime of hundreds of hours for the treatment of relatively clean samples, e.g. single and multiple APIs in a low-electrolyte aqueous medium. For more complex samples, such as food-related wastewater that contains significant concentrations of metal ion chelators, corrosion of the titanium electrodes remains a problem, even after optimisation of the oxide formation, and, for these systems, BDD particle-based feeder electrodes may be required.

### 3.4 Work Package 4: Real-world Wastewater Testing

#### 3.4.1 Task 4.1: wastewater testing at a pharmaceutical production plant, Dublin, Ireland

Dr Declan Moran, Vice President API Development & SRT Strategy at Ipsen, and Dr Sarah Maloney, Head of Environmental Safety and Health at Ipsen, provided insights into the performance characteristics needed for the application of SPy technology within the pharmaceutical industry and identified APIs that have proven especially difficult to treat within their plants worldwide. The applicability of SPy technology to the pharmaceutical industry was investigated in two ways. First, the ability to degrade a range of APIs, including antineoplastic drugs for cancer treatment, NSAIDs and an anticoagulant, was considered. These pharmaceuticals were chosen because they are very difficult to decompose: for example, fluorinated gemcitabine is among the most recalcitrant organic materials. Second, Ipsen provided real-world samples, including “first-wash” and “second-wash” samples from their largest lyophiliser. Our attention focused on correlating reactor performance in the DCU laboratory with synthetic single-component and multicomponent mixtures.

This WP tested the ability of the SPy prototype reactor to decompose a range of recalcitrant organic pharmaceuticals, and the results are described

below. These targets were chosen because of their relevance to the Irish pharmaceutical industry, e.g. the treating of wash and other waste streams used in the production of APIs so that the water can be reused or at least discharged into municipal wastewater, and the significant challenges they pose to traditional multiple-stage treatment processes. These experiments used 2 mm BDD particles and an electric field strength of 30 V cm<sup>-1</sup>; assuming a linear decay of the electric field, the potential drop across the BDD particle would be approximately 6 V and the potential at the anodic pole would approximately 3 V, which is sufficiently positive to generate hydroxy radicals.

#### *Doxorubicin*

Doxorubicin is an anthracycline drug that is used in chemotherapy for a wide range of cancers. It slows or stops the growth of cancer cells by blocking an enzyme called topoisomerase 2, which is required by cancer cells to proliferate and grow. Its structure is shown in Figure 3.30.

Figure 3.31 shows the changes in the UV-Vis spectra of a 0.3 mM solution of doxorubicin dissolved in 0.05 M Na<sub>2</sub>SO<sub>4</sub> following electrolysis for 0, 30, 60, 90 and 120 minutes. These results show that the initial 30 minutes of electrolysis causes the absorbance to decrease by 95%. The TOC value decreases by 80% over this period, suggesting that the majority of the organic carbon is mineralised to CO<sub>2</sub> and water. Significantly, after 90 minutes the absorbance is only 2% ± 1% of the initial value, and diode array HPLC indicates that non-UV-Vis active molecules are present. These results indicate that the BDD particles

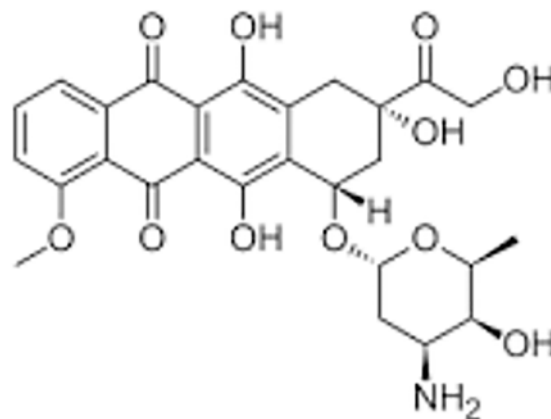


**Figure 3.30. Structure of the anti-neoplastic drug doxorubicin.**

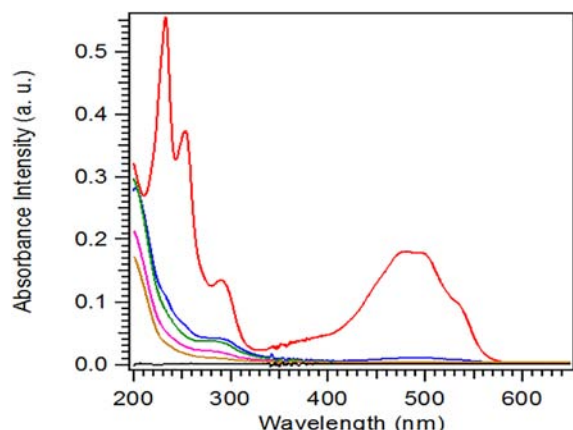


**Figure 3.31. UV-Vis spectra of the blank electrolyte solution, the parent drug doxorubicin and during degradation using electrogenerated hydroxyl radicals. The red line is prior to treatment and the blue, green, pink, brown and black lines are after 1, 2, 3, 4 and 5 hours of treatment using the SPy technology.**

generate hydroxyl radicals that rapidly decompose the recalcitrant doxorubicin, predominantly to  $\text{CO}_2$  and  $\text{H}_2\text{O}$ .

#### Gemcitabine

Gemcitabine is used to treat different cancers, including cancer of the bladder, breast, pancreas and ovary, and non-small cell lung cancer. Its primary mechanism of action is inhibition of DNA synthesis (Sousa *et al.*, 2014). Its structure is shown in Figure 3.32.

Figure 3.33 shows the effects of various electrolysis times on the UV-Vis spectra and HPLC traces for a 1 mM solution of gemcitabine in aqueous 0.05 M

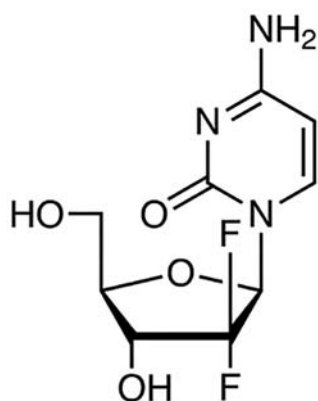


**Figure 3.32. Structure of the anti-cancer drug gemcitabine.**

sodium sulphate solution for periods of up to 3 hours. The UV-Vis intensity decreases systematically as electrolysis proceeds, indicating the decomposition/ decolourisation of the gemcitabine. Significantly, HPLC reveals no evidence of other products being formed that absorb at maximum absorbance wavelength of gemcitabine, suggesting that a significant fraction of the gemcitabine is mineralised to  $\text{CO}_2$ ,  $\text{H}_2\text{O}$  and  $\text{NH}_3$ .

Fluorinated gemcitabine is even more recalcitrant than the parent molecule (Figure 3.34), making it an interesting target for exploring the limits of hydroxyl radicals and the SPy prototype reactor.

Figure 3.35 shows the effects of various electrolysis times on the UV-Vis spectra of fluorinated gemcitabine under the same conditions as those used for gemcitabine (see Figure 3.33). Significantly, while the drug can be decomposed within the SPy reactor, the rate of decomposition for fluorinated gemcitabine is slower than for gemcitabine, reflecting its more recalcitrant nature. Rather than the close to 100% decomposition observed for gemcitabine, only 50% of the fluorinated gemcitabine is decomposed over a 5-hour period.

#### Warfarin

Warfarin is used as an anticoagulant (blood thinner) (Kuruville and Gurk-Turner, 2001). It is commonly used to prevent blood clots such as deep vein thrombosis and pulmonary embolism, and to prevent stroke in people who have atrial fibrillation, valvular heart disease or artificial heart valves. The structure is shown in Figure 3.36.

Solutions of coumadin (containing approximately 10 mM warfarin) were prepared and their decomposition using the SPy prototype reactor investigated. Warfarin is electroactive, and performing SWV on samples taken from the reactor over time is a convenient way to monitor the decomposition of this API and the appearance of electroactive products. Figure 3.37 shows the SWV responses recorded before and after treatment.

Prior to electrolysis, peaks are observed at approximately 0.5 V and 0.8 V, corresponding to the API. These peaks decrease by approximately 50% after 45 minutes of electrolysis, and no detectable quantity (less than  $100 \mu\text{M}$  for SWV) exists after 270 minutes. This result is consistent with hydroxyl

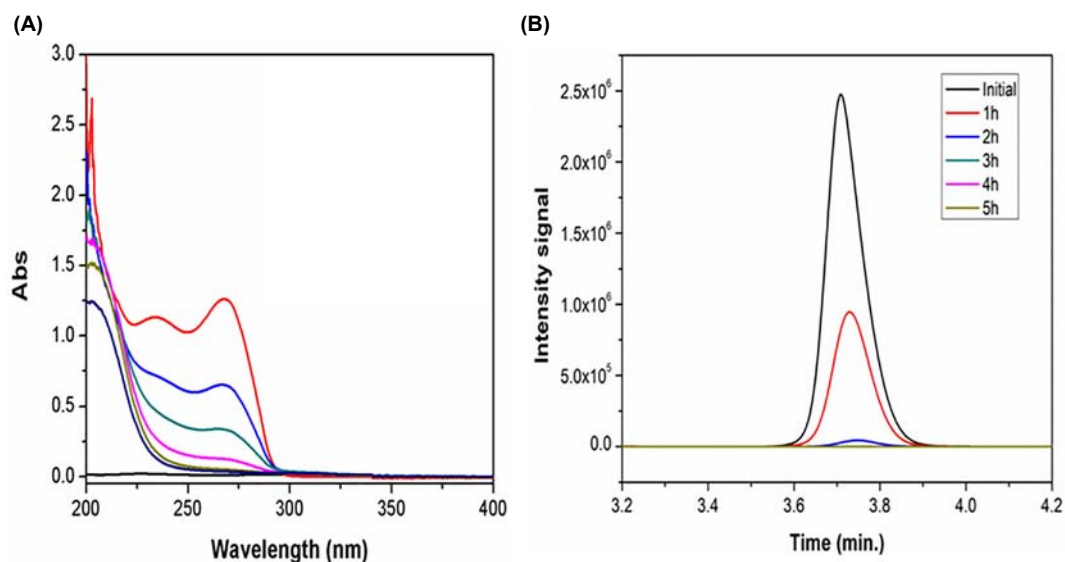


Figure 3.33. Changes in (A) UV-Vis spectra and (B) HPLC traces of a 1 mM solution of gemcitabine following electrolysis in the SPy reactor using BDD particles to wirelessly generate hydroxyl radicals for periods of 0, 1, 2, 3, 4 and 5 hours (top to bottom at 270 nm).

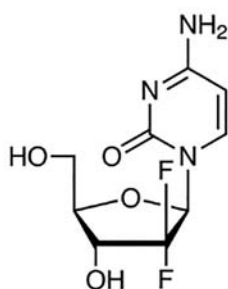


Figure 3.34. Structure of fluorinated gemcitabine.

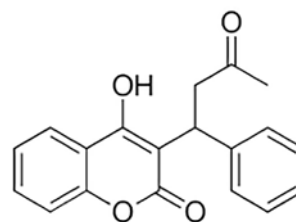


Figure 3.36. Structure of the blood thinner warfarin.

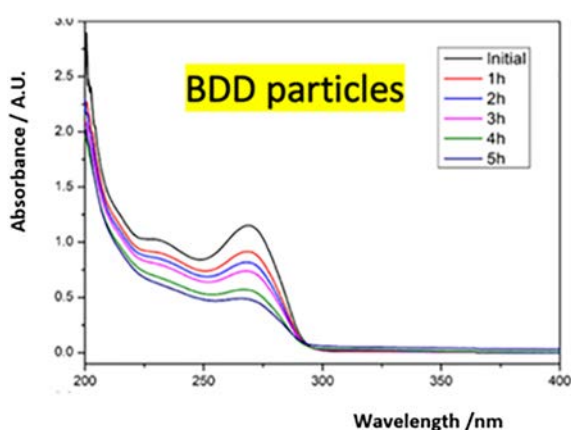
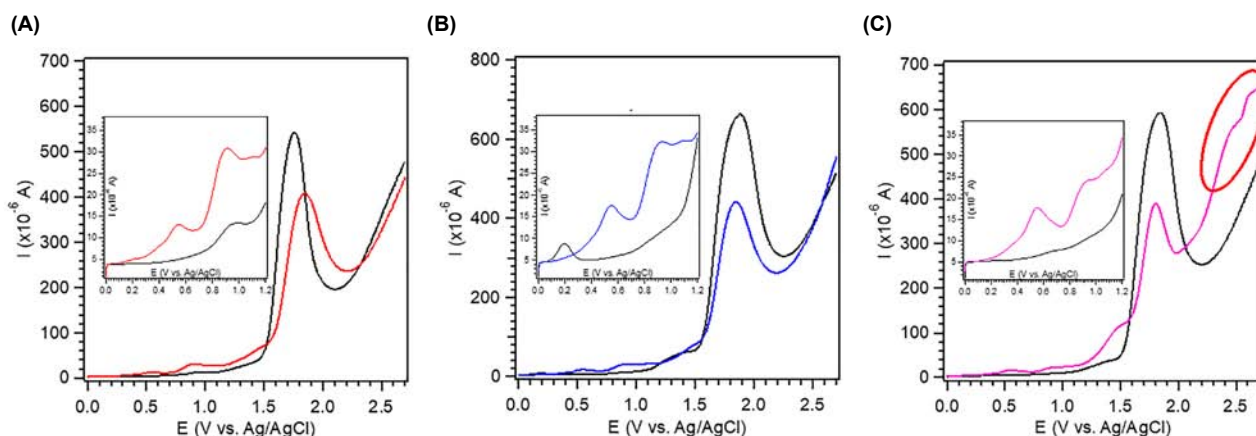


Figure 3.35. Changes in the UV-Vis spectra of a 1 mM solution of fluorinated gemcitabine following electrolysis in the SPy reactor using BDD particles to wirelessly generate hydroxyl radicals for periods of 0, 1, 2, 3, 4 and 5 hours (top to bottom at 270 nm).

radical generation and the degradation of warfarin. HPLC and mass balance data indicate that 75% ± 10% of the organic material is mineralised, with the remainder being low-molecular-weight, non-UV-absorbing, small molecules. These results suggest that the SPy reactor works effectively in the decomposition and partial mineralisation of this fused aromatic ring pharmaceutical.

#### Kinetics of API decomposition

The kinetics of API decomposition have also been investigated for three different recalcitrant drugs: gemcitabine, doxorubicin and cabometyx. As shown in Figure 3.38, SPy technology can decompose solutions of each separate pharmaceutical in less than 5 hours. The different rates of decomposition reflect the different levels of susceptibility of each pharmaceutical



**Figure 3.37.** Electrolysis of coumadin (10 mM warfarin) dissolved in Milli-Q water for (A) 45 minutes, (B) 90 minutes and (C) 270 minutes. The inset shows an expanded view of the peaks at approximately 0.5 V and 0.8 V, corresponding to the API.

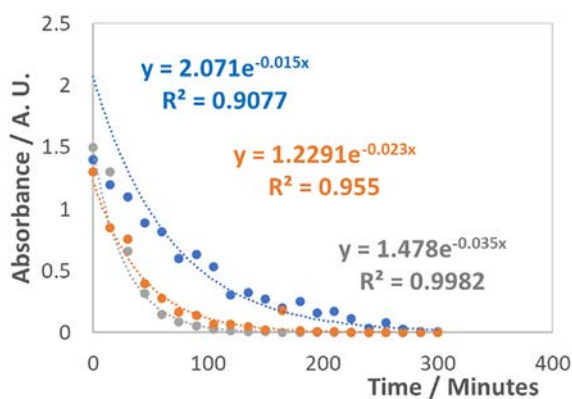


**Figure 3.38.** Decrease in absorbance at 270 nm of a 0.9 mM solution of fluorinated gemcitabine (blue), doxorubicin (orange) and cabometyx (grey) in Milli-Q water over time during wireless electrochemical incineration. BDD particles of 1000 and 500  $\mu\text{m}$  diameter were suspended by stirring into 1 ml samples of the wastewater solution. The voltage difference applied between the two feeder electrodes was 150 V.

to oxidative destruction, as determined by their molecular structure.

#### *Treatment of production wastewater samples*

The programme had access to first- and second-wash samples associated with the production of lanreotide. The SPy reactor showed excellent performance in terms of the mineralisation of lanreotide (with TOC content from 0.1 to 5  $\text{g l}^{-1}$ ). For example, a 4-hour treatment of lanreotide samples (50  $\text{mg ml}^{-1}$ ) resulted in >70% mineralisation and the remaining 30% was

decomposed to simple organic materials. This protocol has been successfully implemented for the treatment of 5 ml samples of first-wash wastewater from the lyophiliser to give purified water samples with no trace (<10  $\mu\text{g ml}^{-1}$ ) of lanreotide (based on UV-Vis and HPLC data) after 4 hours of treatment with the wireless SPy approach. Figure 3.39 shows UV-Vis spectra of the first-wash sample taken after 0, 1, 2 and 3 hours of processing within the SPy reactor. The intensity decreases significantly as the sample is treated, and after 3 hours the absorbance in the visible region becomes zero, with a small residual absorbance (<5% of the initial value) in the UV region that disappears after a further 1 hour of treatment (after 4 hours in total).

Figure 3.40 shows the change in absorbance of a first-wash sample over time. The absorbance shows

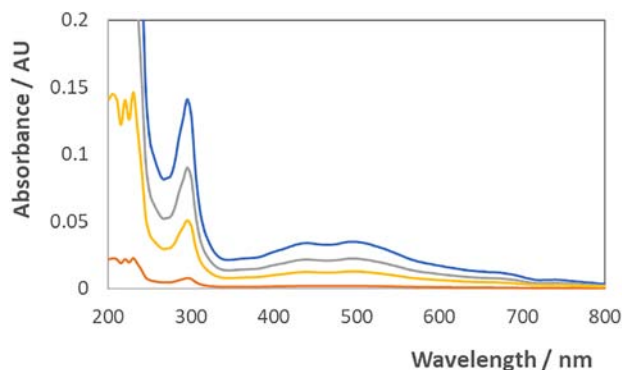


**Figure 3.39.** Changes in the UV-Vis of a first-wash sample following treatment in the SPy reactor for periods of 0, 1, 2 and 3 hours (top to bottom at 500 nm).

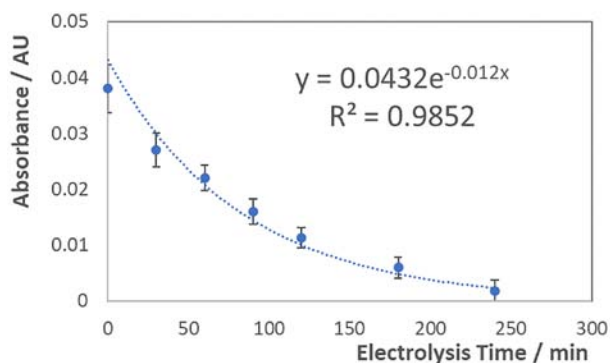


**Figure 3.40.** Changes in absorbance at 550 nm over time during the treatment of a first-wash sample.

a single exponential decay that is consistent with pseudo-first-order kinetics, i.e. there being a significant excess of hydroxyl radicals and their concentration not affecting the rate of decomposition of the organic material. Significantly, the current passed during electrolysis is very low, in  $\text{mAcm}^{-2}$ . This result indicates that each BDD particle acts as a complete electrochemical cell, with hydroxyl radicals being produced at the anode and molecular oxygen and water acting as a sacrificial reductant at the cathode, i.e. very little electricity comes from the power supply. This strategy minimises the current that must be provided externally, making the technology sustainable and a potentially important component of a circular green approach to wastewater treatment.

### Conclusions

Our results suggest that using SPy technology to treat pharmaceutical wastewater to the point that it can be discharged into municipal wastewater treatment systems, or reused within the treatment plant itself, represents an important objective for future development. This is based on (i) the ability of the SPy reactor to rapidly degrade recalcitrant APIs even at relatively modest potentials (65V), (ii) the stability of the titanium feeder electrodes following anodisation,

(iii) the continued high performance and efficiency of the BDD particles over long treatment times, (iv) the stability of the reactor itself and (v) the high margins found in the pharmaceutical sector.

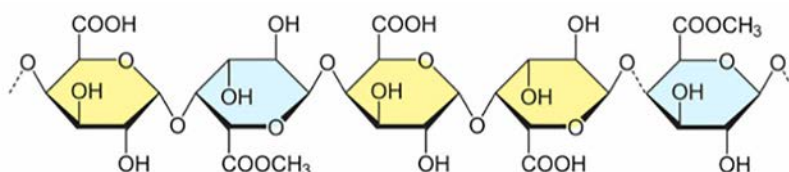
### 3.4.2 Task 4.2: wastewater testing at a food production facility, Nantes, France

Three distinct approaches were used to assess the utility of SPy technology for the treatment of wastewater produced by the food processing industry. First, we used single-component solutions of key target molecules for destruction, e.g. pectin from the processing of fruits and some vegetables. Second, food producer Fleury Michon provided two kinds of samples, one from the direct, untreated wastewater stream from production and a second that had been filtered to remove particulate solids but not otherwise treated. Third, a reactor was shipped to the factory, set up there and tested. The wastewater streams arising from food processing are distinctly different from those from the pharmaceutical industry. They contain a significantly higher organic load, have a wide range of different organic molecules that vary markedly depending on the time of day and with changing seasons, and are poorly characterised.

#### Clean test samples

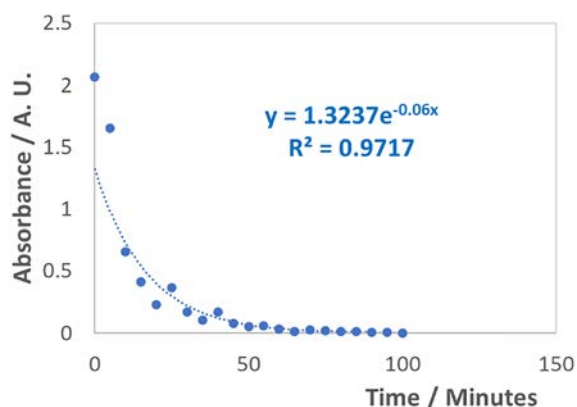
Our partner in the food industry selected pectin (E 440i; see Figure 3.41), a high-molecular-weight carbohydrate polymer found in the cell wall of plants, as the test compound for SPy technology in the context of food production.

Figure 3.42 shows that SPy technology can be used to rapidly decompose pectin, which reflects the high susceptibility of the carbohydrate to the electrogenerated hydroxyl radicals. These data show that the SPy underwater incineration approach effectively decomposes single pollutants relevant to the pharmaceutical and food industries. However,



**Figure 3.41.** Structure of pectin, a significant component of wastewater associated with fruit processing.





**Figure 3.42. Decrease in absorbance at 280 nm of a 10 mM solution of pectin in Milli-Q water over time during wireless electrochemical incineration. BDD particles of 1000 and 500  $\mu\text{m}$  diameter were suspended by stirring into 1 ml samples of the wastewater solution. The voltage difference applied between the two feeder electrodes was 150 V.**

even in this single-component mixture, the current passed during treatment is approximately 10 to 20 times higher, 100 to 200  $\text{mAcm}^{-2}$ , than that for the pharmaceutical samples. This is because the pectin ionises, increasing the conductivity of the medium and causing joule heating of the sample. Moreover, the lifetime of the feeder electrodes is also significantly shorter, at approximately 2.5 hours.

#### *Real-world production samples*

More than 30 wastewater samples were received from Fleury Michon (collected during production and shipped overnight to DCU) that had a TOC content ranging from 0.5 to 100  $\text{g l}^{-1}$ . These samples contained significant quantities of pectin and polyphenols (> 1  $\text{g l}^{-1}$ ), and treating them using BDD particles at 65 V caused the titanium feeder electrodes to oxidise and mechanically deteriorate. The cause of this degradation in the food wastewater samples is the pectin/polyphenols chelating to the Ti or  $\text{Ti}^{2+}$  within the protective oxide coating, causing the protective anodised coating to be removed and exposing the underlying titanium to further oxidative corrosion. Increasing the time used to deposit the oxide layer from 300 to 1000 s at +2 V increased the operational lifetime from 2.5 to 5 hours, because of the increased thickness of the protective oxide coating. However, the formation of the oxide is self-limiting because of its

low electronic conductivity, which prevents the efficient electron transfer needed to form the protective layer.

#### *Placement of reactor in food facility*

With the support of our Joint Programming Initiative collaborator, Professor Yann Pellegrin, the ability of a small-volume prototype SPy reactor to treat waste from Fleury Michon's Nantes site (which produces ready meals) was investigated. The reactor was successfully set up, with the power supply and feeder electrodes working correctly. The reactor was then tested using production wastewater that had a TOC value of between 2 and 10  $\text{g l}^{-1}$ . Voltages of up to 75 V reduced the TOC content of the wastewater by less than 10% over a 3-hour period. This is because the high electrolyte concentration causes the electric field to decay sharply close to the feeder electrode surface, meaning that the voltage induced in the BDD particles is not sufficient to generate hydroxyl radicals. This situation can be addressed by applying a higher voltage to the feeder electrodes. However, the feeder lifetime with these samples at 150 V was very short, approximately 1 hour, before the electrode became physically too fragile (thin) to support further electrolysis. This lack of stability is thought to arise from metal ion chelators within the food samples that bind  $\text{Ti}^{4+}$  ions from the titanium dioxide, causing the protective oxide coating to be removed and exposing the underlying titanium to further oxidative corrosion.

The following five conclusions were reached based on these interactions with Fleury Michon:

1. **Feeder electrodes.** The material used in the feeder electrodes most likely needs to be changed to conducting diamond for it to be sufficiently inert at the very large potentials needed to create a sufficiently intense electric field to wirelessly drive hydroxyl radical generation.
2. **Reactor scale-up.** The scale of Fleury Michon wastewater production is vast, at > 2 million litres per day, and its interest is in systems capable of treating at least 50,000 litres per hour. While outside the scope of the funded programme, we have looked at different reactor designs (predominantly modular, parallel-plate geometry designs with recirculating flow) that could ultimately allow significant volumes of wastewater to be treated. For example, a single

module comprising two 10 cm × 10 cm feeder electrodes with 1 cm separation would preserve the performance of our small prototype reactor, but with a flow rate of 5 ml min<sup>-1</sup>, allowing 500 ml of water containing a recalcitrant organic, e.g. an active API at 10 mg ml<sup>-1</sup>, to be treated in less than 4 hours. Stacks containing multiple copies of these modules would enable relatively large volumes of wastewater to be treated within a meaningful time frame. Fleury Michon has highlighted the need to pay careful attention to issues such as the lifetime and ease of servicing of the seals between the feeder electrodes, separators and housings.

- Maintenance of feeder electrodes.** The ability to quickly replace the feeder electrodes (remove reactor top, slide out old electrode (no (semi-) permanent fixings needed) and slide in the new feeders within 2 minutes) is seen as a design feature that should be preserved in any scaled-up reactor. Fleury Michon highlighted the fact that its in-house maintenance crews would not be able to remove the electrodes and mechanically repolish and re-anodise them before reuse. Therefore, it is essential that future designs feature easily exchanged electrode modules.
- Operator training.** The extent and depth of training required to operate the prototype reactor was considered fully acceptable, with the most significant risk (electrical, due to the high voltages) well addressed by comprehensive insulation.
- BDD particles.** Fleury Michon mentioned some difficulties in handling the BDD particles and achieving a 100% transfer into the reactor. Future designs could place the particles within a porous bag that could be easily placed inside the reactor and still allow the wastewater to come into contact with the particles, allowing the organic materials to be decomposed. In a larger system, cleaning could be performed by pumping the particles out of the system for rinsing and pumping them back after rinsing.

### *Conclusions*

The ability of the SPy approach to treat wastewater generated during food processing in a single stage is complicated by the significant TOC content, the composition changing over time and the chemical

nature of the components, e.g. their ability to complex metals leading to short titanium feeder electrode lifetimes. It is likely that, to create a robust, long-lived and versatile system, non-metal feeder electrodes, e.g. BDD electrodes, will be required. However, the use of BDD electrodes is likely to cause other issues, including higher cost: a 1 cm × 1 cm BDD electrode from a leading manufacturer is €100, and this is the maximum size available.

### **3.4.3 Task 4.3: municipal wastewater treatment testing**

Our work on municipal wastewater took place with our South African collaborator, Professor Emanuel Iwuoha of the University of the Western Cape. The work focused on the detection and decomposition of antiretroviral drugs (ARVs), used for the treatment of HIV, which are typically recalcitrant and not removed by conventional wastewater treatment techniques, such as those using activated sludge and biodegradation. This causes the drugs and their metabolites to accumulate in the environment, making them emerging persistent micropollutants. Figure 3.43A displays the dependence of the differential pulse voltammograms for the ARV nevirapine (NVP) on pH, while the dependence of the peak potential on pH is shown in Figure 3.43B. These results clearly demonstrate that (i) NVP can be irreversibly oxidised (decomposed) at a BDD electrode and (ii) the response depends strongly on the pH of the wastewater sample, with a significantly lower voltage being required as the pH becomes more basic. This behaviour arises because no protons are involved in the electrooxidation of NVP at pH 6–10, while two protons are involved at pH > 10. The proposed mechanism is depicted in Figure 3.44.

### *Conclusions*

These data are encouraging and suggest that ARVs can be both detected and decomposed using electrochemical methods within a BDD-based reactor. However, Covid-19 restrictions in South Africa meant that municipal wastewater samples could not be collected, and the SPy approaches remain untested for real wastewater samples of this type. Moreover, we have concerns about the scalability of the prototype reactor to treat the huge volumes of municipal wastewater produced. For example, we anticipate that

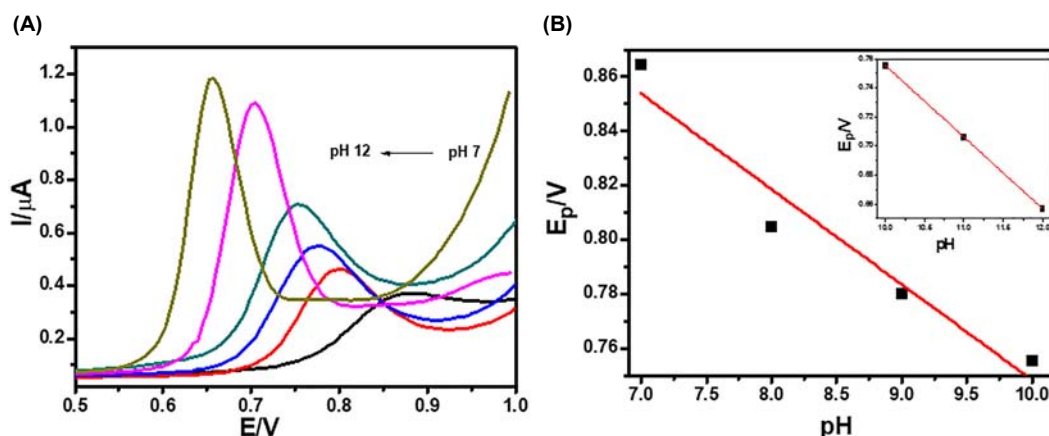


Figure 3.43. (A) Differential pulse voltammograms of 5 µg ml<sup>-1</sup> NVP at different pH values (7–12) recorded in a BDD reactor. (B) Dependence of the peak potential, E<sub>p</sub>, on the solution pH from pH 7 to pH 10 (main) and from pH 10 to pH 12 (inset).

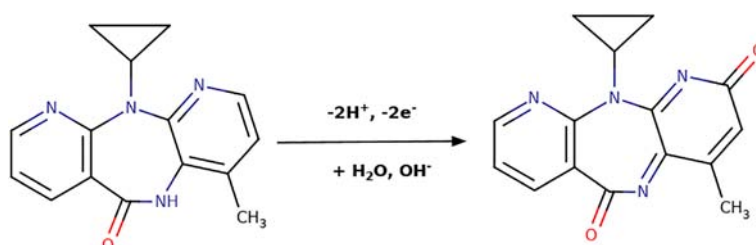


Figure 3.44. Proposed mechanism for electrooxidation of NVP in alkaline media in a BDD reactor.

a stack of 10 10 cm × 10 cm SPy modules with feeder electrodes separated by 1 cm could allow 0.5 litres of NPV-contaminated water to be treated per hour, but this volume is not meaningful within the context of municipal wastewater treatment. Our current data do

not allow us to identify or address scaling issues at higher treatment volumes. Thus, we believe that at this stage of the project's development treating municipal wastewater does not represent the optimum route for further development.



## 4 Conclusions and Policy Recommendations

AOPs are a strongly emerging technology being implemented in wastewater treatment. Electrochemically based methods for producing an active reagent, e.g. hydroxyl radicals, are an important part of the global circular economy. Single AOPs may be used to efficiently purify and treat wastewater. However, complex samples, such as wastewater from food production with a high TOC content, require combinations of AOPs or AOPs to be used in combination with traditional (bio)purification methods. The enhanced performance of combinations of AOPs is mainly due to a higher concentration of free radicals, giving increased oxidation rates, but also because combinations of AOPs modify conditions within the reactor (Gogate and Pandit, 2004). SPy technology could offer the opportunity to use small quantities of sustainably produced electricity to treat industrial wastewater so that it can be reused within the treatment plant (in a circular system) or for other purposes, e.g. agriculture, rather than discharging it into local watercourses or municipal treatment facilities. This approach could help to diminish local water scarcity, with the reuse of reclaimed water being beneficial for the environment. Moreover, the SPy programme has successfully demonstrated that this technology can decompose and mineralise recalcitrant organic pollutants in wastewater that are hazardous to both human beings and aquatic biota.

Perhaps the most significant barrier to the broader application of conventional AOPs is the operating cost per unit mass of organic pollutant eliminated or per unit volume of wastewater treated due to high reagent costs or significant power consumption. SPy technology solves this issue by having each BDD particle act as a separate electrochemical cell in which oxygen or water is reduced, acting as a sink for electrons removed from water, which are used to generate hydroxyl radicals. Therefore, under ideal conditions, no power is consumed to drive the electrolysis; power is consumed only to establish the electric field. In practice, where there is no electrolyte, or the samples contain very little electrolyte, e.g. pharmaceutical samples, the current consumed

by the SPy reactor is in the order of a few  $\text{mAcm}^{-2}$ . However, for more conducting solutions, e.g. food waste, the current is significantly higher because of joule heating of the solution. The most significant challenge is the scalability of the technology, e.g. the costs of large surface area feeder electrodes and BDD particles.

A 30-page report has been generated titled *Market Possibilities for Technology and Initial Assessment of Route to Market*. The aim of the report was to provide an initial perspective on the commercial possibilities for SPy technology and to identify a potentially effective route to market. It identified the following key benefits of SPy technology:

- It provides a more cost-effective approach to wastewater treatment through lower operating expenses, primarily through enhanced energy efficiency using a wireless electrochemical oxidation process.
- It is more environmentally friendly than other processes, since no additional chemicals need to be added and the active species does not leave a chemical residue.
- It is implementable at source and highly portable.

### 4.1 Target Markets Identified

The following potential target markets were identified:

- **Pharmaceutical.** The outlook for the use of SPy technology in the pharmaceutical industry is positive, as indirect competitors provide access to numerous markets and clients. Moreover, only limited resources would need to be rolled out to facilitate expansion of the use of the technology in a very large and growing sector.
- **Food processing.** This would be a difficult market to penetrate with SPy technology because of the complexities of wastewater treatment in the sector.
- **Municipal.** Municipal wastewater treatment is heavily regulated, and the data needed to conduct a cost-benefit analysis of rolling out SPy technology in this sector are lacking.

Overall, SPy technology may be considered advantageous in the current context of increasingly stringent water regulations, the pollution of water

resources from agricultural and industrial activities and the requirement that industry meet effluent discharge standards.

# References

- Ciríaco, L., Anjo, C., Correia, J., Pacheco, M. and Lopes, A., 2009. Electrochemical degradation of ibuprofen on Ti/Pt/PbO<sub>2</sub> and Si/BDD electrodes. *Electrochimica Acta* 54: 1464–1472.
- Garcia-Costa, A.L., Alves, A., Madeira, L.M. and Santos, M.S., 2021. Oxidation processes for cytostatic drugs elimination in aqueous phase: a critical review. *Journal of Environmental Chemical Engineering* 9: 104709.
- Gogate, P.R. and Pandit, A.B., 2004. A review of imperative technologies for wastewater treatment II: hybrid methods. *Advances in Environmental Research* 8: 553–597.
- Katheresan, V., Kansedo, J. and Lau, S.Y., 2018. Efficiency of various recent wastewater dye removal methods: a review. *Journal of Environmental Chemical Engineering* 6: 4676–4696.
- Kuruvilla, M. and Gurk-Turner, C., 2001. A review of warfarin dosing and monitoring. *Baylor University Medical Center Proceedings* 14(3): 305–306.
- Miklos, D.B., Remy, C., Jekel, M., Linden, K.G., Drewes, J.E. and Hübner, U., 2018. Evaluation of advanced oxidation processes for water and wastewater treatment – a critical review. *Water Research* 139: 118–131.
- Pavlos K., Pandis, C., Kalogirou, E., Kanellou, E., Vaitsis, C., Savvidou, M.G., Sourkouni, G., Zorpas, A.A. and Argirusis, C., 2022. Key points of advanced oxidation processes (AOPs) for wastewater, organic pollutants and pharmaceutical waste treatment: a mini review. *Chemical Engineering* 6: 8.
- Prousek, J., 1996. Advanced oxidation processes for water treatment. Chemical processes. *Chemické Listy* 90: 229–237.
- Sillanpää, M., Ncibi, M.C. and Matilainen, A., 2018. Advanced oxidation processes for the removal of natural organic matter from drinking water sources: a comprehensive review. *Journal of Environmental Management* 208: 56–76.
- Sousa, L., Cavalcante, G. and Monteiro, G., 2014. Gemcitabine: metabolism and molecular mechanisms of action, sensitivity and chemoresistance in pancreatic cancer. *European Journal of Pharmacology* 741: 8–16.
- Vlyssides, A., Papaioannou, D., Loizidou, M., Karlis, P.K. and Zorpas, A.A., 2000. Testing an electrochemical method for treatment of textile dye wastewater. *Waste Management* 20: 569–576.
- Zhang, J., Zhou, Y., Yao, B., Yang, J. and Zhi, D., 2021. Current progress in electrochemical anodic-oxidation of pharmaceuticals: mechanisms, influencing factors, and new technique. *Journal of Hazardous Materials* 418: 126313.

# Abbreviations

<b>ABS</b>	Acrylonitrile butadiene styrene
<b>AOP</b>	Advanced oxidation process
<b>API</b>	Active pharmaceutical ingredient
<b>ARV</b>	Antiretroviral drug
<b>BDD</b>	Boron-doped diamond
<b>CAD</b>	Computer-aided design
<b>CFU</b>	Colony-forming unit
<b>DCU</b>	Dublin City University
<b>ECL</b>	Electrochemiluminescence
<b>FITC</b>	Fluorescein isothiocyanate
<b>HPLC</b>	High-performance liquid chromatography
<b>LOD</b>	Limit of detection
<b>NIPAM</b>	<i>N</i> -isopropylacrylamide
<b>NSAID</b>	Non-steroidal anti-inflammatory drug
<b>NVP</b>	Nevirapine
<b>PETG</b>	Polyethylene terephthalate glycol-modified
<b>PLA</b>	Polylactic acid
<b>SPy</b>	Sense and Purify
<b>SWV</b>	Square wave voltammetry
<b>TOC</b>	Total organic carbon
<b>WHO</b>	World Health Organization
<b>WP</b>	Work package
<b>7OHC</b>	7-Hydroxycoumarin

# An Gníomhaireacht Um Chaomhnú Comhshaoil

Tá an GCC freagrach as an gcomhshaoil a chosaint agus a fheabhsú, mar shócmhainn luachmhar do mhuintir na hÉireann. Táimid tiomanta do dhaoine agus don chomhshaoil a chosaint ar thionchar díobhálach na radaíochta agus an truaillithe.

## Is féidir obair na Gníomhaireachta a roinnt ina trí phríomhréimse:

**Rialáil:** Rialáil agus córais chomhlíonta comhshaoil éifeachtacha a chur i bhfeidhm, chun dea-thorthaí comhshaoil a bhaint amach agus díriú orthu siúd nach mbíonn ag cloí leo.

**Eolas:** Sonraí, eolas agus measúnú ardchaighdeán, spriocdhírthe agus tráthúil a chur ar fáil i leith an chomhshaoil chun bonn eolais a chur faoin gcinnteoireacht.

**Abhcóideacht:** Ag obair le daoine eile ar son timpeallachta glaine, táirgiúla agus dea-chosanta agus ar son cleachtas inbhuanaithe i dtaobh an chomhshaoil.

## I measc ár gcuid freagrachtaí tá:

### Ceadúnú

- > Gníomhaíochtaí tionscail, dramhaíola agus stórála peitрил ar scála mór;
- > Sceitheadh fuíolluisce uirbhig;
- > Úsáid shrianta agus scaoileadh rialaithe Orgánach Géinmhodhnaithe;
- > Foinsí radaíochta ianúcháin;
- > Astaíochtaí gás ceaptha teasa ó thionscal agus ón eitlíocht trí Scéim an AE um Thrádáil Astaíochtaí.

### Forfheidhmiú Náisiúnta i leith Cúrsaí Comhshaoil

- > Iniúchadh agus cigireacht ar shaoráidí a bhfuil ceadúnas acu ón GCC;
- > Cur i bhfeidhm an dea-chleachtais a stiúradh i ngníomhaíochtaí agus i saoráidí rialáilte;
- > Maoirseacht a dhéanamh ar fhreagrachtaí an údaráis áitiúil as cosaint an chomhshaoil;
- > Caighdeán an uisce óil phoiblí a rialáil agus údaruithe um sceitheadh fuíolluisce uirbhig a fhorfheidhmiú
- > Caighdeán an uisce óil phoiblí agus phríobháidigh a mheasúnú agus tuairisciú air;
- > Comhordú a dhéanamh ar líonra d'eagraíochtaí seirbhíse poiblí chun tacú le gníomhú i gcoinne coireachta comhshaoil;
- > An dlí a chur orthu siúd a bhriseann dlí an chomhshaoil agus a dhéanann dochar don chomhshaoil.

### Bainistíocht Dramhaíola agus Ceimiceáin sa Chomhshaoil

- > Rialacháin dramhaíola a chur i bhfeidhm agus a fhorfheidhmiú lena n-áirítear saincheisteanna forfheidhmithe náisiúnta;
- > Staitisticí dramhaíola náisiúnta a ullmhú agus a fhoilsiú chomh maith leis an bPlean Náisiúnta um Bainistíocht Dramhaíola Guaisí;
- > An Clár Náisiúnta um Chosc Dramhaíola a fhorbairt agus a chur i bhfeidhm;
- > Reachtaíocht ar rialú ceimiceáin sa timpeallacht a chur i bhfeidhm agus tuairisciú ar an reachtaíocht sin.

### Bainistíocht Uisce

- > Plé le struchtúir náisiúnta agus réigiúnacha rialachais agus oibriúcháin chun an Chreat-treoir Uisce a chur i bhfeidhm;
- > Monatóireacht, measúnú agus tuairisciú a dhéanamh ar chaighdeán aibhneacha, lochanna, uiscí idirchreasa agus cósta, uiscí snámha agus screamhuisce chomh maith le tomhas ar leibhéal uisce agus sreabhadh abhann.

### Eolaíocht Aeráide & Athrú Aeráide

- > Fardail agus réamh-mheastacháin a fhoilsiú um astaíochtaí gás ceaptha teasa na hÉireann;
- > Rúnaíocht a chur ar fáil don Chomhairle Chomhairleach ar Athrú Aeráide agus tacaíocht a thabhairt don Idirphlé Náisiúnta ar Gníomhú ar son na hAeráide;

- > Tacú le gníomhaíochtaí forbartha Náisiúnta, AE agus NA um Eolaíocht agus Beartas Aeráide.

### Monatóireacht & Measúnú ar an gComhshaoil

- > Córais náisiúnta um monatóireacht an chomhshaoil a cheapadh agus a chur i bhfeidhm: teicneolaíocht, bainistíocht sonraí, anailís agus réamhaisnéisiú;
- > Tuairiscí ar Staid Thimpeallacht na hÉireann agus ar Tháscairí a chur ar fáil;
- > Monatóireacht a dhéanamh ar chaighdeán an aeir agus Treoir an AE i leith Aeir Ghlain don Eoraip a chur i bhfeidhm chomh maith leis an gCoinbhinsiún ar Aerthruailliú Fadraoin Trasteorann, agus an Treoir i leith na Teorann Náisiúnta Astaíochtaí;
- > Maoirseacht a dhéanamh ar chur i bhfeidhm na Treorach i leith Torainn Timpeallachta;
- > Measúnú a dhéanamh ar thionchar pleananna agus clár beartaithe ar chomhshaoil na hÉireann.

### Taighde agus Forbairt Comhshaoil

- > Comhordú a dhéanamh ar ghníomhaíochtaí taighde comhshaoil agus iad a mhaoiniú chun brú a aithint, bonn eolais a chur faoin mbeartas agus réitigh a chur ar fáil;
- > Comhoibriú le gníomhaíocht náisiúnta agus AE um thaighde comhshaoil.

### Cosaint Raideolaíoch

- > Monatóireacht a dhéanamh ar leibhéal radaíochta agus nochtadh an phobail do radaíocht ianúcháin agus do réimsí leictreamaighnéadacha a mheas;
- > Cabhrú le pleananna náisiúnta a fhorbairt le haghaidh éigeandálaí ag eascairt as tasmí núicléacha;
- > Monatóireacht a dhéanamh ar fhorbairtí thar lear a bhaineann le saoráidí núicléacha agus leis an tsábháilteacht raideolaíochta;
- > Sainseirbhísí um chosaint ar an radaíocht a sholáthar, nó maoirsiú a dhéanamh ar sholáthar na seirbhísí sin.

### Treoir, Ardú Feasachta agus Faisnéis Inrochtana

- > Tuairisciú, comhairle agus treoir neamhspleách, fianaise-bhunaithe a chur ar fáil don Rialtas, don tionscal agus don phobal ar ábhair maidir le cosaint comhshaoil agus raideolaíoch;
- > An nasc idir sláinte agus folláine, an geilleagar agus timpeallacht ghlan a chur chun cinn;
- > Feasacht comhshaoil a chur chun cinn lena n-áirítear tacú le hiompraíocht um éifeachtúlacht acmhainní agus aistriú aeráide;
- > Tástáil radóin a chur chun cinn i dtithe agus in ionaid oibre agus feabhsúchán a mholadh áit is gá.

### Comhpháirtíocht agus Líonrú

- > Oibriú le gníomhaireachtaí idirnáisiúnta agus náisiúnta, údaráis réigiúnacha agus áitiúla, eagraíochtaí neamhrialtais, comhlachtaí ionadaíochta agus ranna rialtais chun cosaint comhshaoil agus raideolaíoch a chur ar fáil, chomh maith le taighde, comhordú agus cinnteoireacht bunaithe ar an eolaíocht.

## Bainistíocht agus struchtúr na Gníomhaireachta um Chaomhnú Comhshaoil

Tá an GCC á bainistiú ag Bord lánaimseartha, ar a bhfuil Ard-Stiúrthóir agus cúigear Stiúrthóir. Déantar an obair ar fud cúig cinn d'Oifigí:

1. An Oifig um Inbhuanaitheacht i leith Cúrsaí Comhshaoil
2. An Oifig Forfheidhmithe i leith Cúrsaí Comhshaoil
3. An Oifig um Fhianaise agus Measúnú
4. An Oifig um Chosaint ar Radaíocht agus Monatóireacht Comhshaoil
5. An Oifig Cumarsáide agus Seirbhísí Corparáideacha

Tugann coistí comhairleacha cabhair don Gníomhaireacht agus tagann siad le chéile go rialta le plé a dhéanamh ar ábhair inmí agus le comhairle a chur ar an mBord.

## EPA Research

**Webpages:** [www.epa.ie/our-services/research/](http://www.epa.ie/our-services/research/)

**LinkedIn:** [www.linkedin.com/showcase/eparesearch/](http://www.linkedin.com/showcase/eparesearch/)

**Twitter:** @EPAResearchNews

**Email:** [research@epa.ie](mailto:research@epa.ie)